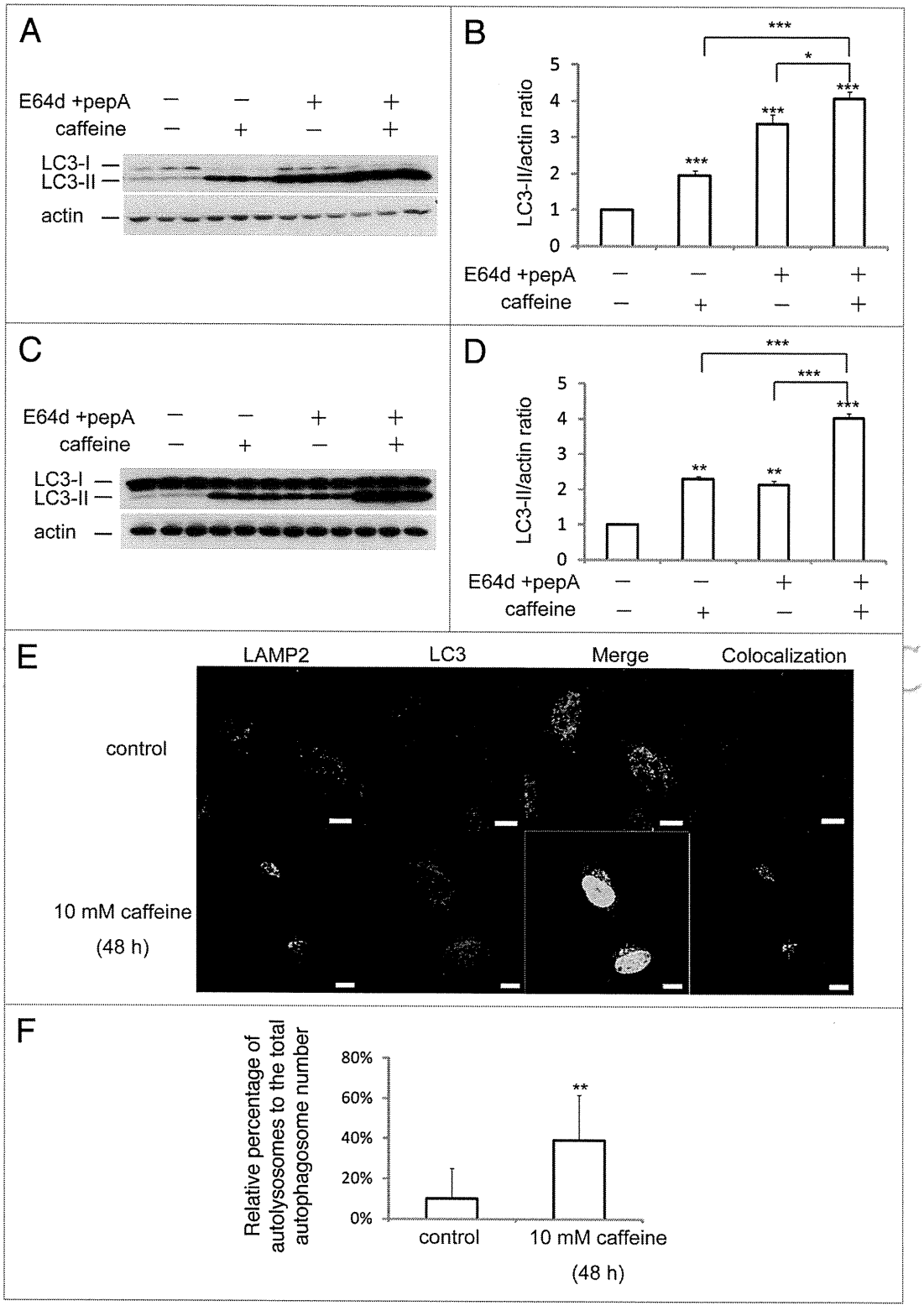


**Figure 2.** Caffeine does not block autophagosome-lysosome fusion. (A–D) SH-SY5Y (A) or HeLa (C) cells treated with 10 mM caffeine with or without E64d (10 μg/ml) and pepstatin A (10 μg/ml) were analyzed by immunoblotting with antibodies against LC3 and actin. Densitometry analysis of LC3 levels relative to actin in SH-SY5Y (B) and HeLa (D) cells was performed using three independent experiments. (E and F) HeLa cells treated with various concentrations of caffeine for 48 hours were analyzed using confocal microscopy (E). Number of the autolysosomes and autophagosomes were automatically counted using ImageJ "Colocalization" Plugin and the ratios were calculated (F).

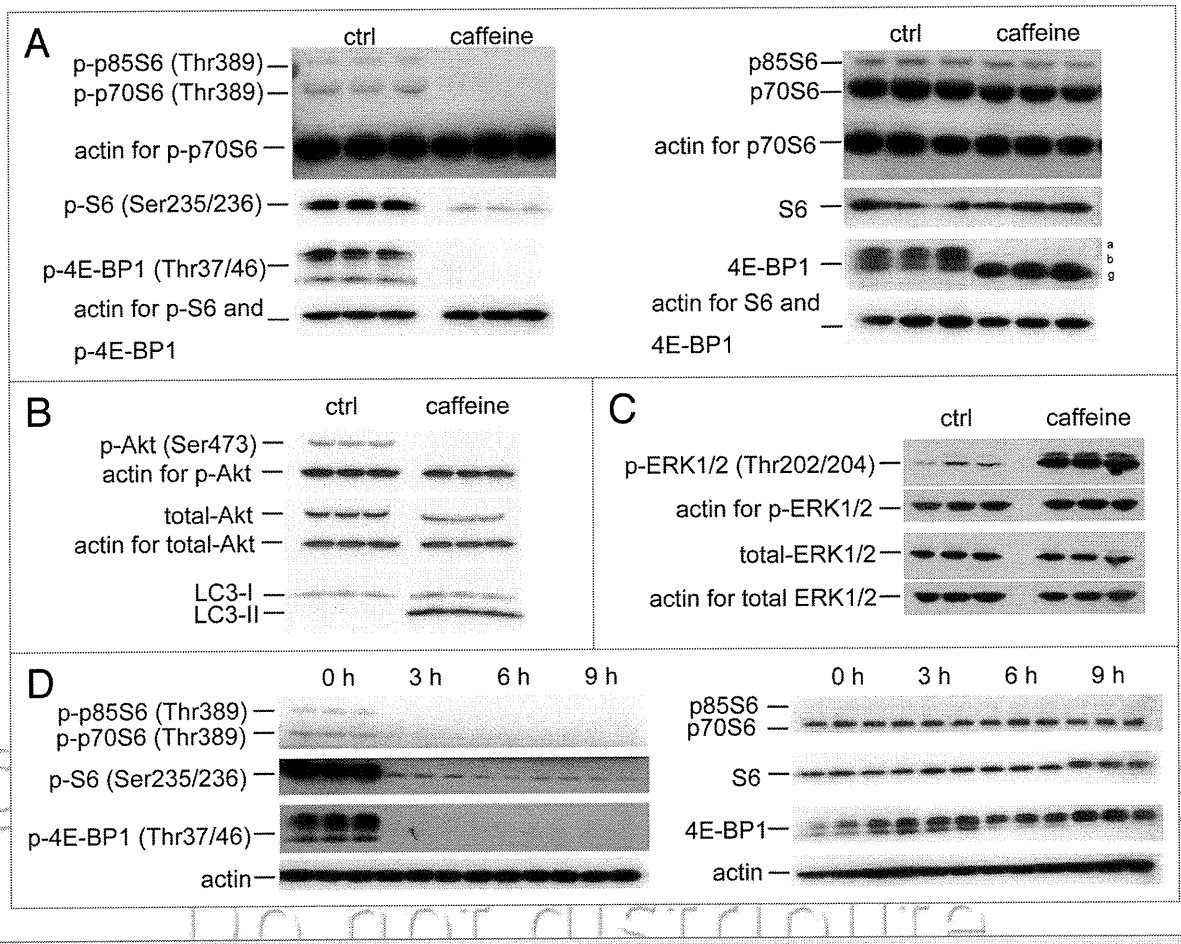


**Figure 3.** Caffeine inhibits the Akt/mTOR/p70S6 signaling pathway and activates ERK1/2 signaling. (A and B) SH-SY5Y cells treated with or without 10 mM caffeine for 24 hours were analyzed for mTOR activity by immunoblotting for levels of phosphor- and total p70 ribosomal S6 protein, S6, 4E-BP1 (A), Akt (B) and actin. (C) SH-SY5Y cells treated with or without 10 mM caffeine for 0, 3, 6 or 9 hours were analyzed by immunoblotting for levels of phosphor- and total ERK1/2 and actin. (D) SH-SY5Y cells treated with 10 mM caffeine for various time periods were analyzed by immunoblotting for levels of phosphor- and total p70 ribosomal S6 protein, S6, 4E-BP1 and actin.

increased the percentage of cells in the sub-$G_1$ peak, which is indicative of apoptosis (**Fig. 6C**). To confirm whether caffeine-induced cell death is apoptotic, we examined the activity of caspase-3, a well-known inducer of apoptosis. Treatment with 10 mM caffeine markedly increased levels of cleaved caspase-3 and decreased full-length caspase-3 in PC12D cells (**Fig. 6D**), consistent with previous reports on the induction of apoptosis by caffeine.[35-37]

To test whether caffeine-induced apoptosis is dependent on autophagy, we determined whether the inhibition of autophagy by 3-methyladenine (3-MA) or Atg7 siRNA knockdown affects caffeine-induced cytotoxicity in PC12D cells. Treatment with 1 or 5 mM 3MA or Atg7 knockdown significantly decreased the percentage of cell death or cells with reduced mitochondrial membrane potentials caused by caffeine treatment (5 or 10 mM) (**Fig. 6E and F and Suppl. Fig. S6B**). As can be seen from the increased caffeine-induced apoptosis shown in **Figure 6A and C**, our data suggests that caffeine-induced autophagy is necessary for apoptotic cell death. To further confirm this, we compared autophagy-deficient mouse embryonic fibroblasts (MEFs), lacking the Atg7 gene ($Atg7^{-/-}$), without LC3-II expression (**Suppl. Fig. S4E**), and matched wild-type ($Atg7^{+/+}$) MEFs, in which autophagy is induced by caffeine in a dose-dependent manner (**Suppl. Fig. S4C and D**). As expected, the level of caffeine-induced cell death (positive to trypan blue staining) in $Atg7^{-/-}$ MEFs was less than that in $Atg7^{+/+}$ MEFs (**Fig. 7A**). The numbers of early apoptotic cells (annexin V positive, PI negative) were significantly increased in both a time-dependent and dose-dependent manner by caffeine treatment of $Atg7^{+/+}$ MEFs compared to $Atg7^{-/-}$ MEFs (**Fig. 7B–D**). Also, apoptotic or necrotic cells (annexin V positive) were significantly increased by caffeine treatment of $Atg7^{+/+}$ MEFs compared to $Atg7^{-/-}$ MEFs (**Suppl. Fig. S6**). Together, these results indicate that caffeine-induced autophagy partly occurs upstream of apoptosis and is not a protective response to caffeine.

In various tumor cell lines, higher concentrations of caffeine alone induce p53-dependent $G_1$ phase arrest and under certain conditions apoptosis can also occur in a p53-independent manner.[1] Furthermore, disruption at the $G_2$/M checkpoint by caffeine allows cells time to repair DNA damage by driving them through mitosis, eventually resulting in apoptosis.[36,38,39] Consistent with these reports, the results of our study indicate that increased

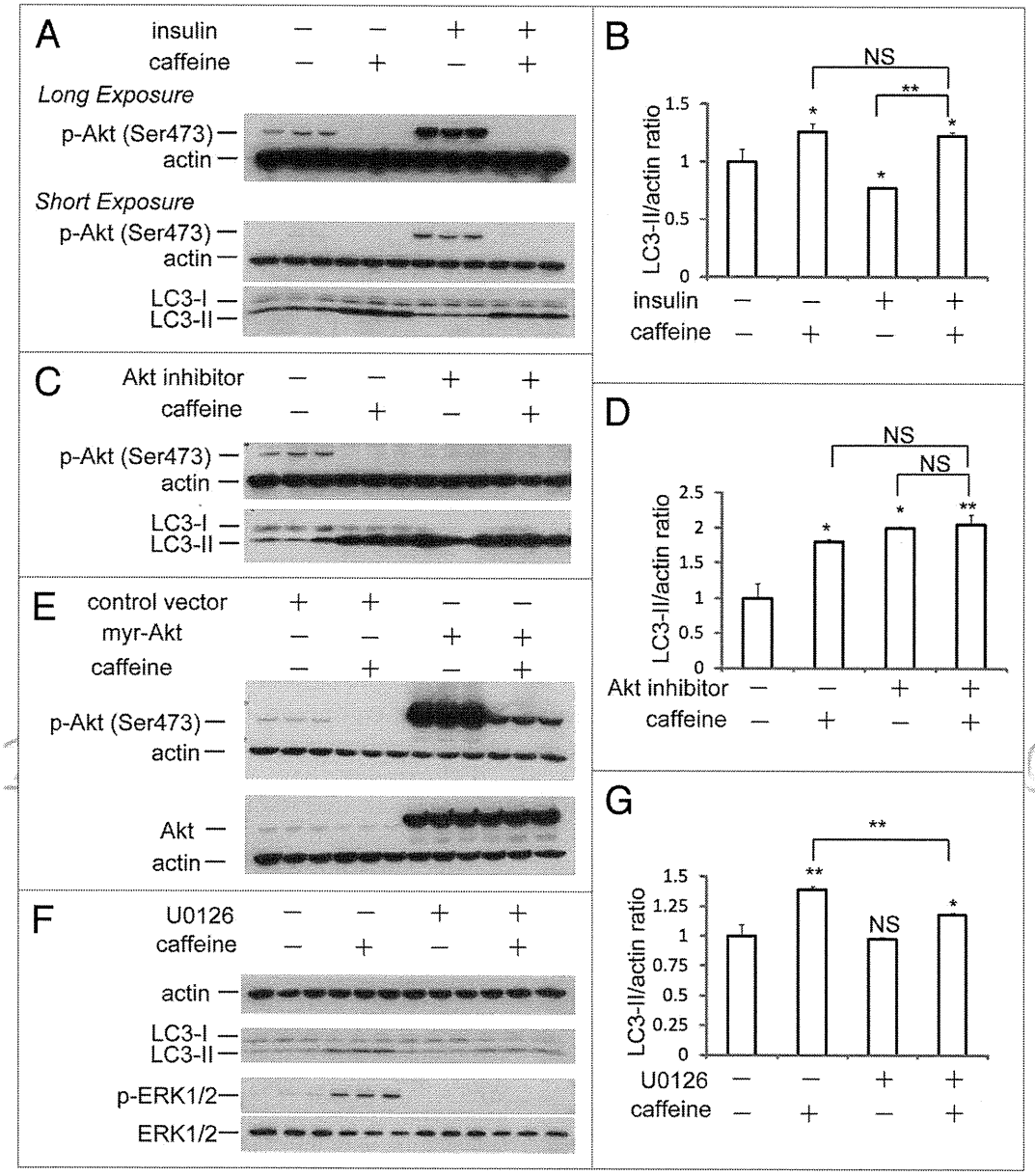


**Figure 4.** Caffeine-induced autophagy is dependent on PI3K/Akt/mTOR pathway. (A) SH-SY5Y cells treated with 25 mM caffeine for 3 hours followed by treatment with or without 200 nM insulin for 30 minutes were analyzed by immunoblotting. (B) Densitometry analysis of LC3-II levels relative to actin was performed using three independent experiments. (C) SH-SY5Y cells treated with 25 mM caffeine, 50 μM Akt1/2 inhibitors or 25 mM caffeine with 50 μM Akt1/2 inhibitors for 6 hours were analyzed by immunoblotting. (D) Densitometry analysis of LC3-II levels relative to actin was performed using three independent experiments. (E) SH-SY5Y cells were transfected for 24 hours with either a control plasmid DNA (pcDNA3.1) or a plasmid encoding constitutively active Akt (myr-Akt), and then treated with $H_2O$ or 10 mM caffeine for 6 hours. Immunoblotting was performed using antibodies against Akt, p-Akt (Ser 473) and actin. (F) SH-SY5Y cells treated with 25 mM caffeine with or without 20 μM U0126 for 6 hours were analyzed by immunoblotting using antibodies against actin, LC3, p-ERK and ERK. (G) Densitometry analysis was performed using three independent experiments. Error bars, SD; *$p < 0.05$; **$p < 0.01$; N.S., not significant.

concentrations of caffeine treatment cause a dose-dependent increase in apoptosis. More recently, autophagy, a process long known to provide a survival advantage to cells undergoing nutrient deprivation and other stresses, has also been linked to the cell death process.[7] The cross-talk between apoptosis and autophagy is complex and sometimes contradictory; however, it is critical to the overall fate of the cell. In this study, we have shown that autophagy is induced by higher concentrations of caffeine without starvation, mainly via the inhibition of PI3K/Akt/mTOR/p70S6K signaling. Likewise, when caffeine-induced autophagy is blocked by 3-MA treatment or Atg7 knockout, apoptosis is partially attenuated, suggesting that caffeine-induced autophagy occurs upstream of caffeine-induced apoptosis. It also indicates the involvement of other pathways in caffeine-induced apoptosis. These results provide new insight into the effects of caffeine on cell death and survival and its use as a possible

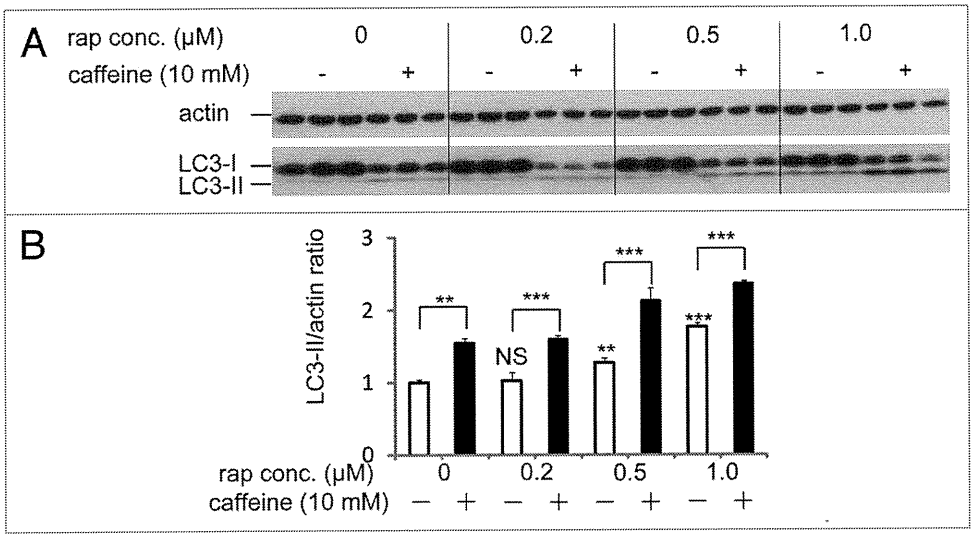


**Figure 5.** Rapamycin treatment with caffeine has an additive effect on enhancement of autophagy. (A) SH-SY5Y cells treated with various concentrations of rapamycin with or without 10 mM caffeine for 48 hours were analyzed by immunoblotting. (B) Densitometry analysis was performed using three independent experiments. Error bars, SD; *p < 0.05; **p < 0.01; N.S., not significant.

intervention strategy for the upregulation of apoptosis by a harnessing of its autophagic activity in tumor treatment.

## Materials and Methods

**Cell line.** HeLa cells were maintained in DMEM (Sigma) supplemented with 10% fetal bovine serum (FBS) (Sigma) and 100 U/ml penicillin/streptomycin (Sigma) at 37°C and 5% $CO_2$. PC12D and SH-SY5Y cells were maintained in DMEM (Sigma) supplemented with 10% FBS (Sigma), 5% horse serum and 100 U/ml penicillin/streptomycin at 37°C and 5% $CO_2$. All experiments with PC12D were performed after differentiation with NGF treatment for 48 hours. $Atg7^{+/+}$ and $^{-/-}$ MEFs were maintained in DMEM (Sigma) supplemented with 10% FBS, 100 U/ml penicillin/streptomycin, 1% sodium pyruvate (Gibco, 11360), 1% non-essential amino acid (NEAA) and 4.2 μl 2% beta-mercaptoethanol at 37°C.

To establish a HeLa GFP-LC3 stable cell line, proliferating HeLa cells were transfected with a GFP-LC3 plasmid.[14] Forty-eight hours post-transfection with Lipofectamine 2000 (Invitrogen), positive stable clones were selected by growing cells with G418 (400 μg/ml) for 2 weeks and maintained in DMEM (Sigma) supplemented with 10% FBS (Sigma), 100 U/ml penicillin/streptomycin and 200 μg/ml G418 at 37°C and 5% $CO_2$. All cellular experiments were performed with cells cultured in complete medium with FBS as explained above.

**Cell viability assays.** A trypan blue dye (Invitrogen, 15250-061) exclusion assay was used to examine cell viability and performed according to previously reported protocols.[40,41] Changes of mitochondrial membrane potentials were assessed also with the lipophilic cationic membrane-potential-sensitive dye JC-1 (5,5',6,6'-tetrachloro-1,1',3,3'-tetrachylbenzimidazolylcarbocyanineiodide) (Wako, 106-00131) according to the manufacturer's protocol. Detection of early apoptotic cells was determined using an annexin V/propidium iodide (PI) detection kit (Invitrogen), according to the manufacturer's protocol. Briefly, 0.5 x $10^6$ $Atg7^{+/+}$ or $^{-/-}$ MEFs were exposed to caffeine (0–25 mM) for 24 hours and washed twice. Then, they were incubated at room temperature with annexin V/Alexa488 and PI for 15 minutes. Annexin $V^+PI^-$ cells, considered as early apoptotic cells, were enumerated using FACScan (BD Biosciences). Data were analyzed with CellQuest (BD Biosciences) and FlowJo softwares (Tree Star Inc.). Cells positive or negative for annexin V were regarded as apoptotic or non-apoptotic cells, respectively.

**Cell cycle analysis.** To examine apoptosis, 1.0 x $10^4$ cells/well PC12D cells were seeded onto 96-well culture plate and incubated for 48 h in DMEM with NGF and treated with caffeine for 72 h. The cells were harvested and washed with PBS and

**Figure 6 (See opposite page).** Caffeine induces apoptosis by enhancement of autophagy. (A) After PC12D cells were treated with 0, 1, 2.5, 5 or 10 mM caffeine with DMSO or $MPP^+$ for 72 hours, cell viability was measured using trypan blue dye exclusion assay. Data are the means of triplicate experiments. (B) After cells were treated with 0, 1, 2.5, 5 or 10 mM caffeine with DMSO or $MPP^+$ for 48 hours, mitochondrial membrane potential was analyzed by JC-1 using a flow cytometry. Data are the means of triplicate experiments. (C) After PC12D cells were treated with 0, 1, 2.5, 5 or 10 mM caffeine with DMSO or $MPP^+$ for 72 hours, caffeine-induced sub $G_1$ area was analyzed by propidium iodide staining assay using a flow cytometry. Data are the means of triplicate experiments. (D) PC12D cells were treated with $H_2O$ or caffeine for 24 hours or staurosporine (positive control) for 3 hours and analyzed with immunoblotting for levels of caspase-3 and cleaved caspase-3. (E) After PC12D cells were treated with 0, 1, 2.5, 5 or 10 mM caffeine with or without 1, 3 or 5 mM 3MA for 24 hours, cell viability was measured by trypan blue dye exclusion assay. (F) PC12D cells were transfected with control siRNA or siRNAs targeting Atg7. Forty eight hours later, they were treated with 0, 1, 2.5 or 10 mM caffeine for 24 hours and mitochondrial membrane potential was analyzed using JC-1. The knockdown effects on Atg7 were confirmed by immunoblotting using antibodies against Atg7 and actin. Data are the means of triplicate experiments. Error bars, S.D. NS, not significant; *p < 0.05; **p < 0.01; ***p < 0.001.

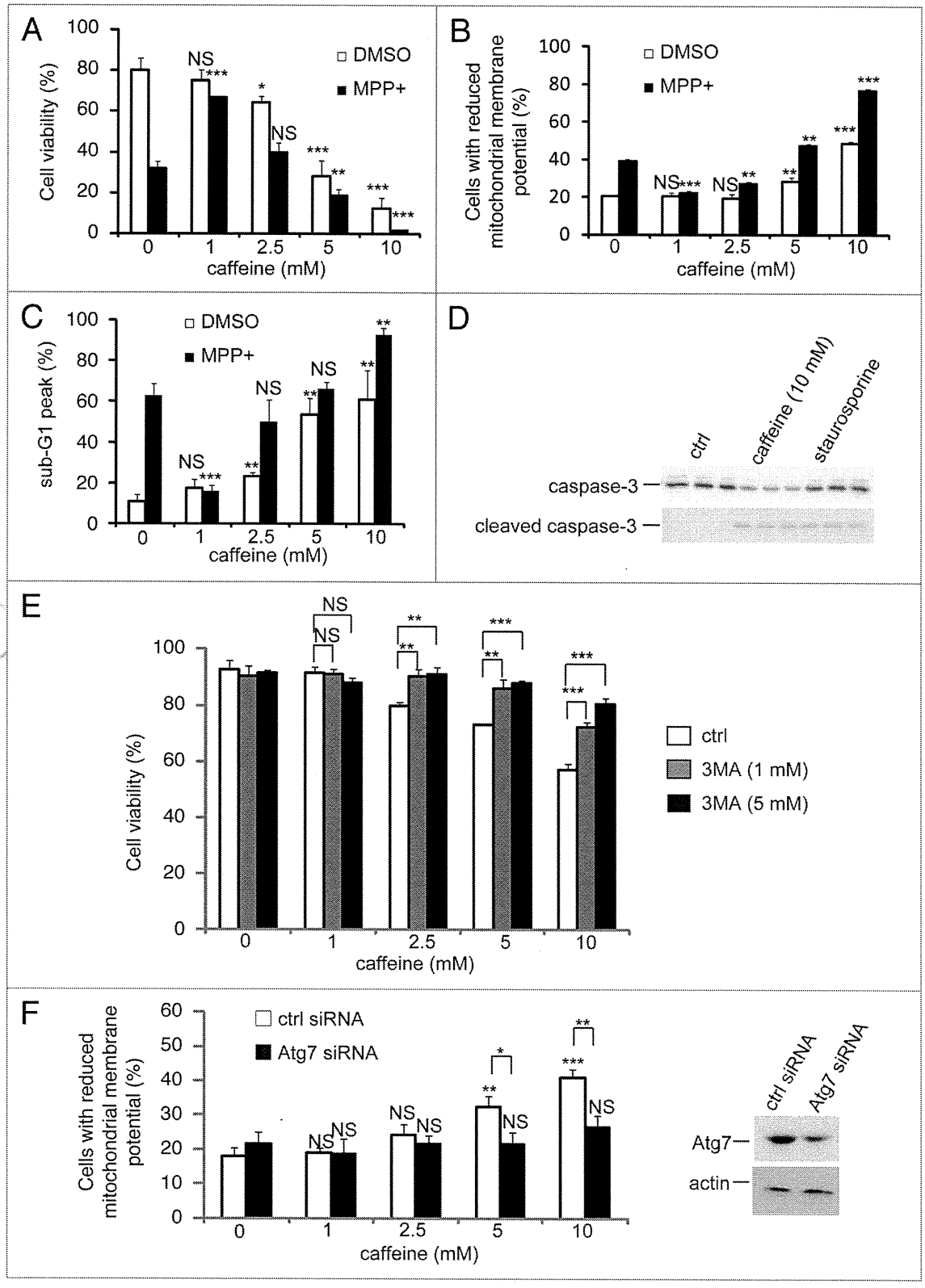


fixed with ice-cold 70% ethanol at 4°C for 2 h. The cells were then stained with PI solution according to previously reported protocol.[41] DNA content was analyzed by flow cytometry using FACScan and CellQuest software (BD Biosciences).

**Compounds.** Compounds used included caffeine (Wako, 031-06792), E64d (Sigma, E8640), pepstatin A (Sigma, P5318), rapamycin (LC Laboratories, R5000), CCI-779 (Selleck Chemicals, S1044), MPP+ (Sigma, M0896), bafilomycin A1 (Sigma, B1793), 3-methyladenine (Sigma, M9281), insulin (Sigma, I0516), U0126 (Sigma, U120), Akt1/2 inhibitors (Sigma, A6730), staurosporine (Cell Signaling Technology, 9953) and DMSO (Sigma, D2650).

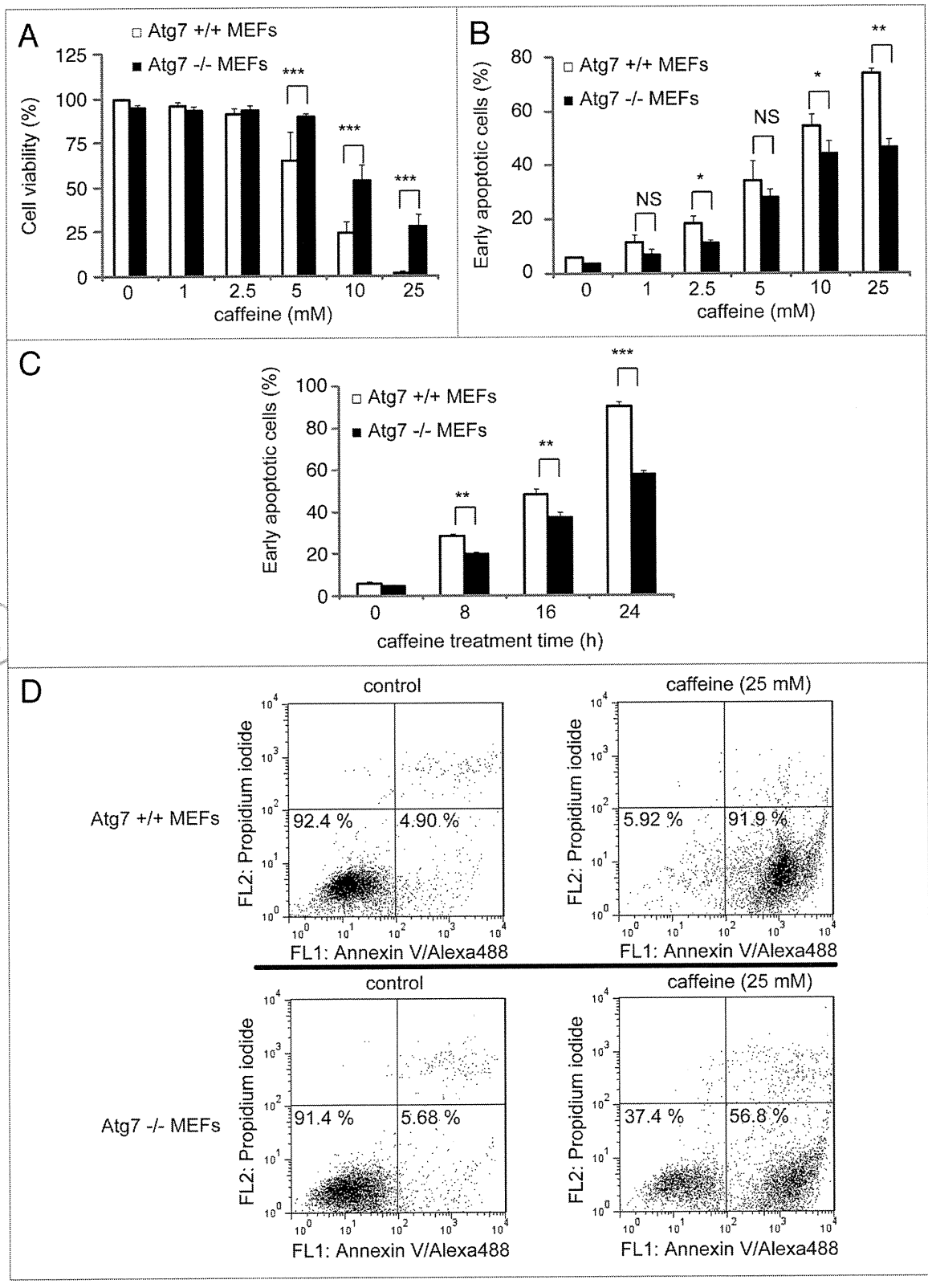


**Figure 7.** Cells without Atg7 expression are more resistant to caffeine-induced apoptosis. (A) After Atg7$^{+/+}$ or $^{-/-}$ mouse embryonic fibroblasts (MEFs) were treated with 0, 1, 2.5, 5, 10, 25 mM caffeine for 24 hours, the cell viability was measured by trypan blue dye exclusion assay. Data are the means of triplicate experiments. (B–D) Fluorescence-activated cell-sorting analysis for annexin V/propidium iodide (PI). Atg7$^{+/+}$ or $^{-/-}$ MEFs were cultured with various concentrations of caffeine for 24 hours (B) or with 25 mM caffeine for various times (0, 8, 16 or 24 hours) (C and D). Annexin V/PI staining was subsequently performed to assess early or late apoptosis and necrosis. 5 x $10^3$ cells were analyzed by flow cytometry and the percentage of early apoptotic cells (annexin V-positive and PI-negative cells, the lower right region in (D) was determined). Data are the means of triplicate experiments. Error bars, SD. NS, not significant; *$p < 0.05$; **$p < 0.01$; ***$p < 0.001$.

**Plasmid DNAs.** Myrystoylated Akt (21–151), a constitutively active form of Akt, was purchased from Millipore.

*siRNA knockdown experiments.* PC12D cells were transfected with rat Atg7 siRNAs (Invitrogen, 10620318-9) using Lipofectamine RNAiMAX (Invitrogen, 13778-075) according to the manufacturer's protocol.

**Western blotting.** Cell pellets were lysed on ice in RIPA buffer for 20 minutes in the presence of protease inhibitor (Roche). Western blotting was performed according to a previously published report.[42] The antibodies used were as follows: anti-p70 ribosomal protein (Cell Signaling Technology, 2708), anti-ribosomal protein (Cell Signaling Technology, 2217), anti-4E-BP1 (Cell Signaling Technology, 9452), anti-Akt (Cell Signaling Technology, 9272), anti-p44/42 MAP kinase (Cell Signaling Technology, 9102), anti-phospho-p70 ribosomal protein (Thr389) (Cell Signaling Technology, 9205), anti-phospho-S6 ribosomal protein (Ser235/236) (Cell Signaling Technology, 2211), anti-phospho-4E-BP1 (Thr37/46) (Cell Signaling Technology, 9459), anti-phospho-p44/p42 MAPK (Thy202/Tyr204) (Cell Signaling Technology, 9101), anti-Atg7 (Cell Signaling Technology, 2631), anti-phospho-Akt (Cell Signaling Technology, 4060), anti-actin (Millipore, clone C4), anti-LC3 (MBL, clone 4E12), anti-p62 (Progen Biotechnik, GP62-C) antibodies. Antibody signals were enhanced with chemifluorescent methods from GE HealthCare.

**Immunofluorescent microscopy.** Cells were embedded with 4% paraformaldehyde for 20 minutes. Following this, they were permeabilized with 0.1% Triton-X in 1x PBS. After incubation with 10% FBS and 1% bovine serum albumin in 1x PBS for 30 minutes, cells were immunostained with anti-LC3B (x500) (Sigma, L7543), anti-LAMP2 (x50) (Development Studies Hybridoma Bank, clone H4B4) overnight and incubated with anti-rabbit IgG tagged with AlexaFluor 488 or anti-mouse IgG tagged with AlexaFluor 546 for 1 hour. The cover slips were embedded with VectaShield, stained with DAPI and images were acquired on a Zeiss LSM510 META confocal microscope (63 x 1.4 NA) or a Leica TCS SP5 confocal microscope at room temperature using Zeiss LSM510 v.3.2 software or Leica LAS AF software. Adobe Photoshop 7.0 (Adobe Systems Inc.) was used for subsequent image processing. For colocalization assay in HeLa cells, an appropriate confocal image was taken with Leica LAS AF software. Then, these images were analyzed automatically with the ImageJ "Colocalization" Plugin (Settings: Each threshold: 25, Ratio: 75%) followed by "Analyze particles" (Settings: threshold 25; Pixel: 1) between endogenous LC3 positive and LAMP2 vesicles. Experiments were done in triplicate at least twice.

**Quantification of cells with GFP-LC3 vesicles.** HeLa cells stable expressing GFP-LC3 were treated with various concentrations of caffeine for 24 or 48 hours and then fixed as described above. Analyses in triplicate were done for counting the proportion of GFP-positive cells with GFP-LC3 vesicles as previously described in reference 43.

**Electron microscopy.** SH-SY5Y cells treated with various concentrations of caffeine were prefixed in 2% glutaraldehyde in PBS at 4°C, treated with 1% $OsO_4$ for 3 hours at 4°C, dehydrated in a graded series of ethanol and flat embedded in epon. Ultra-thin sections were doubly stained with uranyl acetate and observed using a JEOL JEM-2000EX electron microscopy at 80 kV.

**Statistical analysis.** Densitometry analysis was performed using ImageJ 1.43 on immunoblots from three independent experiments. A t-test was performed with SYSTAT software (Hulinks).



### Acknowledgements

We thank Dr. Takashi Ueno (Department of Biochemistry, Juntendo University) for critical comments and Drs. Masaaki Komatsu and Yu-Shin Sou for providing $Atg7^{+/+}$ and $^{-/-}$ MEFs. We are very grateful for a grant from Hayashi Memorial Foundation for Female Natural Scientists (Y.S.), the Grant-in-Aid for Young Scientists (B) (S. Saiki and F. Sato), grants from the All Japan Coffee Association (S. Saiki), the Takeda Scientific Foundation (S. Saiki) and the Nagao Memorial Fund (S. Saiki).

### Note

Supplementary materials can be found at:
www.landesbioscience.com/supplement/SaikiAUTO7-2-Sup.pdf

### References

1. Bode AM, Dong Z. The enigmatic effects of caffeine in cell cycle and cancer. Cancer Lett 2007; 247:26-39.
2. Jang MH, Shin MC, Kang IS, Baik HH, Cho YH, Chu JP, et al. Caffeine induces apoptosis in human neuroblastoma cell line SK-N-MC. J Korean Med Sci 2002; 17:674-8.
3. Gururajanna B, Al-Katib AA, Li YW, Aranha O, Vaitkevicius VK, Sarkar FH. Molecular effects of taxol and caffeine on pancreatic cancer cells. Int J Mol Med 1999; 4:501-7.
4. Qi W, Qiao D, Martinez JD. Caffeine induces TP53-independent G(1)-phase arrest and apoptosis in human lung tumor cells in a dose-dependent manner. Radiat Res 2002; 157:166-74.
5. Mizushima N, Levine B, Cuervo AM, Klionsky DJ. Autophagy fights disease through cellular self-digestion. Nature 2008; 451:1069-75.
6. Rubinsztein DC. The roles of intracellular protein-degradation pathways in neurodegeneration. Nature 2006; 443:780-6.
7. Eisenberg-Lerner A, Bialik S, Simon HU, Kimchi A. Life and death partners: apoptosis, autophagy and the cross-talk between them. Cell Death Differ 2009; 16:966-75.
8. Espert L, Denizot M, Grimaldi M, Robert-Hebmann V, Gay B, Varbanov M, et al. Autophagy is involved in T cell death after binding of HIV-1 envelope proteins to CXCR4. J Clin Invest 2006; 116:2161-72.
9. Foukas LC, Daniele N, Ktori C, Anderson KE, Jensen J, Shepherd PR. Direct effects of caffeine and theophylline on p110delta and other phosphoinositide 3-kinases. Differential effects on lipid kinase and protein kinase activities. J Biol Chem 2002; 277:37124-30.
10. Kudchodkar SB, Yu Y, Maguire TG, Alwine JC. Human cytomegalovirus infection alters the substrate specificities and rapamycin sensitivities of raptor- and rictor-containing complexes. Proc Natl Acad Sci USA 2006; 103:14182-7.
11. Winter G, Hazan R, Bakalinsky AT, Abeliovich H. Caffeine induces macroautophagy and confers a cytocidal effect on food spoilage yeast in combination with benzoic acid. Autophagy 2008; 4:28-36.
12. Rubinsztein DC, Cuervo AM, Ravikumar B, Sarkar S, Korolchuk V, Kaushik S, Klionsky DJ. In search of an "autophagomometer". Autophagy 2009; 5:585-9.
13. Tanida I, Ueno T, Kominami E. LC3 and Autophagy. Methods Mol Biol 2008; 445:77-88.
14. Kabeya Y, Mizushima N, Ueno T, Yamamoto A, Kirisako T, Noda T, et al. LC3, a mammalian homologue of yeast Apg8p, is localized in autophagosome membranes after processing. EMBO J 2000; 19:5720-8.
15. Yamamoto A, Tagawa Y, Yoshimori T, Moriyama Y, Masaki R, Tashiro Y. Bafilomycin A1 prevents maturation of autophagic vacuoles by inhibiting fusion between autophagosomes and lysosomes in rat hepatoma cell line, H-4-II-E cells. Cell Struct Funct 1998; 23:33-42.
16. Mizushima N, Yoshimori T, Levine B. Methods in mammalian autophagy research. Cell 140:313-26.
17. Hanahan D, Weinberg RA. The hallmarks of cancer. Cell 2000; 100:57-70.
18. Ikenoue T, Hong S, Inoki K. Monitoring mammalian target of rapamycin (mTOR) activity. Methods Enzymol 2009; 452:165-80.

19. Sinn B, Tallen G, Schroeder G, Grassl B, Schulze J, Budach V, Tinhofer I. Caffeine confers radiosensitization of PTEN-deficient malignant glioma cells by enhancing ionizing radiation-induced $G_1$ arrest and negatively regulating Akt phosphorylation. Mol Cancer Ther 9:480-8.
20. Sarkaria JN, Busby EC, Tibbetts RS, Roos P, Taya Y, Karnitz LM, Abraham RT. Inhibition of ATM and ATR kinase activities by the radiosensitizing agent, caffeine. Cancer Res 1999; 59:4375-82.
21. Inoki K, Li Y, Xu T, Guan KL. Rheb GTPase is a direct target of TSC2 GAP activity and regulates mTOR signaling. Genes Dev 2003; 17:1829-34.
22. Inoki K, Li Y, Zhu T, Wu J, Guan KL. TSC2 is phosphorylated and inhibited by Akt and suppresses mTOR signalling. Nat Cell Biol 2002; 4:648-57.
23. Garami A, Zwartkruis FJ, Nobukuni T, Joaquin M, Roccio M, Stocker H, et al. Insulin activation of Rheb, a mediator of mTOR/S6K/4E-BP signaling, is inhibited by TSC1 and 2. Mol Cell 2003; 11:1457-66.
24. Muise-Helmericks RC, Grimes HL, Bellacosa A, Malstrom SE, Tsichlis PN, Rosen N. Cyclin D expression is controlled post-transcriptionally via a phosphatidylinositol-3-kinase/Akt-dependent pathway. J Biol Chem 1998; 273:29864-72.
25. Degtyarev M, De Maziere A, Orr C, Lin J, Lee BB, Tien JY, et al. Akt inhibition promotes autophagy and sensitizes PTEN-null tumors to lysosomotropic agents. J Cell Biol 2008; 183:101-16.
26. Wan X, Harkavy B, Shen N, Grohar P, Helman LJ. Rapamycin induces feedback activation of Akt signaling through an IGF-1R-dependent mechanism. Oncogene 2007; 26:1932-40.
27. Sun SY, Rosenberg LM, Wang X, Zhou Z, Yue P, Fu H, Khuri FR. Activation of Akt and eIF4E survival pathways by rapamycin-mediated mammalian target of rapamycin inhibition. Cancer Res 2005; 65:7052-8.
28. O'Reilly KE, Rojo F, She QB, Solit D, Mills GB, Smith D, et al. mTOR inhibition induces upstream receptor tyrosine kinase signaling and activates Akt. Cancer Res 2006; 66:1500-8.
29. Cirstea D, Hideshima T, Rodig S, Santo L, Pozzi S, Vallet S, et al. Dual inhibition of akt/mammalian target of rapamycin pathway by nanoparticle albumin-bound-rapamycin and perifosine induces antitumor activity in multiple myeloma. Mol Cancer Ther 2010; 9:963-75.
30. Aoki H, Takada Y, Kondo S, Sawaya R, Aggarwal BB, Kondo Y. Evidence that curcumin suppresses the growth of malignant gliomas in vitro and in vivo through induction of autophagy: role of Akt and extracellular signal-regulated kinase signaling pathways. Mol Pharmacol 2007; 72:29-39.
31. Ellington AA, Berhow MA, Singletary KW. Inhibition of Akt signaling and enhanced ERK1/2 activity are involved in induction of macroautophagy by triterpenoid B-group soyasaponins in colon cancer cells. Carcinogenesis 2006; 27:298-306.
32. Rubinsztein DC, Gestwicki JE, Murphy LO, Klionsky DJ. Potential therapeutic applications of autophagy. Nat Rev Drug Discov 2007; 6:304-12.
33. Ravikumar B, Vacher C, Berger Z, Davies JE, Luo S, Oroz LG, et al. Inhibition of mTOR induces autophagy and reduces toxicity of polyglutamine expansions in fly and mouse models of Huntington disease. Nat Genet 2004; 36:585-95.
34. Kotake Y, Ohta S. $MPP^+$ analogs acting on mitochondria and inducing neuro-degeneration. Curr Med Chem 2003; 10:2507-16.
35. Hagan MP, Hopcia KL, Sylvester FC, Held KD. Caffeine-induced apoptosis reveals a persistent lesion after treatment with bromodeoxyuridine and ultraviolet-B light. Radiat Res 1997; 147:674-9.
36. Efferth T, Fabry U, Glatte P, Osieka R. Expression of apoptosis-related oncoproteins and modulation of apoptosis by caffeine in human leukemic cells. J Cancer Res Clin Oncol 1995; 121:648-56.
37. Shinomiya N, Takemura T, Iwamoto K, Rokutanda M. Caffeine induces S-phase apoptosis in cis-diamminedichloroplatinum-treated cells, whereas cis-diamminedichloroplatinum induces a block in $G_2$/M. Cytometry 1997; 27:365-73.
38. Lau CC, Pardee AB. Mechanism by which caffeine potentiates lethality of nitrogen mustard. Proc Natl Acad Sci USA 1982; 79:2942-6.
39. Takagi M, Shigeta T, Asada M, Iwata S, Nakazawa S, Kanke Y, et al. DNA damage-associated cell cycle and cell death control is differentially modulated by caffeine in clones with p53 mutations. Leukemia 1999; 13:70-7.
40. Ormerod MG, Collins MK, Rodriguez-Tarduchy G, Robertson D. Apoptosis in interleukin-3-dependent haemopoietic cells. Quantification by two flow cytometric methods. J Immunol Methods 1992; 153:57-65.
41. Kawatani M, Uchi M, Simizu S, Osada H, Imoto M. Transmembrane domain of Bcl-2 is required for inhibition of ceramide synthesis, but not cytochrome *c* release in the pathway of inostamycin-induced apoptosis. Exp Cell Res 2003; 286:57-66.
42. Kawajiri S, Saiki S, Sato S, Sato F, Hatano T, Eguchi H, Hattori N. PINK1 is recruited to mitochondria with parkin and associates with LC3 in mitophagy. FEBS Lett 2010; 584:1073-9.
43. Sarkar S, Davies JE, Huang Z, Tunnacliffe A, Rubinsztein DC. Trehalose, a novel mTOR-independent autophagy enhancer, accelerates the clearance of mutant huntingtin and alpha-synuclein. J Biol Chem 2007; 282:5641-52.

JNNP Online First, published on December 3, 2011 as 10.1136/jnnp-2011-301205


REVIEW

# Molecular pathogenesis of Parkinson's disease: update

Shinji Saiki, Shigeto Sato, Nobutaka Hattori

Department of Neurology, Juntendo University School of Medicine, Bunkyo, Tokyo, Japan

**Correspondence to**
Professor N Hattori, Department of Neurology, Juntendo University School of Medicine, 2-1-1 Hongo, Bunkyo-ku, Tokyo 113-8421, Japan; nhattori@juntendo.ac.jp

Received 16 August 2011
Revised 6 November 2011
Accepted 9 November 2011

## ABSTRACT

Parkinson disease (PD) is a neurodegenerative disease characterised by progressive disturbances in motor, autonomic and psychiatric functions. Much has been learnt since the disease entity was established in 1817. Although there are well established treatments that can alleviate the symptoms of PD, a pressing need exists to improve our understanding of the pathogenesis to enable development of disease modifying treatments. Ten responsible genes for PD have been identified and recent progress in molecular research on the protein functions of the genes provides new insights into the pathogenesis of hereditary as well as sporadic PD. Also, genome wide association studies, a powerful approach to identify weak effects of common genetic variants in common diseases, have identified a number of new possible PD associated genes, including PD genes previously detected. However, there is still much to learn about the interactions of the gene products, and important insights may come from chemical and genetic screens. In this review, an overview is provided of the molecular pathogenesis and genetics of PD, focusing particularly on the functions of the PD related gene products with marked research progress.

## INTRODUCTION

Parkinson's disease (PD) is the second most common progressive neurodegenerative disease, named after James Parkinson's who provided a classic account of the condition in 1817. Affecting 1–2% of the population over the age of 65 years, the prevalence of PD increases by approximately 4% in those older than 85 years. Ten genes that contribute to the genetic aetiology of hereditary PD (hPD) were identified, mainly through positional cloning strategies in inherited PD patients and families (table 1).[1 2] Several responsible genes for hPD have been identified, and based on functional studies in vitro and in vivo of gene products, some have been found to interact with each other in various cellular systems for homeostasis, such as synaptic homeostasis (α-synuclein), mitochondrial maintenance (PINK1, parkin, DJ-1, Omi/HtrA2), autophagy–lysosome pathway (α-synuclein, parkin, PINK1, Omi/HtrA2), axonal transport (LRRK2) and ubiquitin proteasome systems (α-synuclein, parkin, DJ-1, UCH-L1). Impairments in a number of cellular systems have been suggested to underlie hPD (figure 1). Also, more recent studies revealed that mutations in the same genes can be involved in familial PD and be risk factors for sporadic PD (sPD), suggesting that inherited and sPD could have common pathological mechanisms.[3] Therefore, understanding the function of the proteins encoded by hPD genes will hopefully further our understanding of the mechanisms leading to inherited and sPD.

In this review, we will summarise the latest research progress in the molecular mechanisms of hPD and genetic association studies of sPD.

## HEREDITARY PD

### α-Synuclein (PARK1 and PARK4)

#### Clinicogenetics

*SNCA* was the first causal PD gene identified in a large Italian family.[4] Mutations (A30P, E46K and A53T), duplications and triplications of the *SNCA* gene have been reported.[2] Clinical features of patients with the E46K mutation are similar to those of dementia with Lewy bodies, while A30P is not associated with severe dementia. Individuals with *SNCA* triplication developed an early onset form of PD with rapid progression and more extended neurodegeneration.[5]

Recent genome wide association studies (GWAS) have demonstrated a strong association between common single nucleotide polymorphism within the *SNCA* locus and PD in European and Japanese population, consistent with the finding that variation at the *SNCA* locus increases PD susceptibility.[6–9] Although the *SNCA* single nucleotide polymorphism associated with sPD show a low OR (1.2–1.4), these findings are consistent with α-synuclein aggregation pathology.

#### Molecular biology

α-Synuclein is mainly expressed in the presynaptic terminal of the CNS. The protein binds with lipids and unfolds in the steady state. Although the exact function remains unclear, it regulates dopamine homeostasis in presynaptic vesicle cycling.[5] The phenotype of α-synuclein knockout mice is unremarkable and only shows a mild decrease in dopamine levels in the striatum and a mild decrease in synaptic vesicles in the hippocampus. Compared with the wild-type α-synuclein, mutant forms easily aggregate in neuronal cells in vitro and in vivo.[10 11] Transgenic mice with wild or mutant α-synuclein under various promoters have shown neuronal inclusions, mitochondrial abnormalities and neurodegeneration.[12–14] Which type of α-synuclein species is the most toxic to cells remains unclear but some studies assert that mature aggregates are not themselves the toxic moiety but rather an attempt by the cell to clear small toxic oligomers.[15] Hsp90 modulates the assembly of α-synuclein in an ATP

**Table 1** Genetic and clinical characteristics of hereditary Parkinson's disease

| Locus | Inheritance | Gene | Type of mutation | Clinical features |
|---|---|---|---|---|
| PARK1/PARK4 | AD | SNCA | Missense, duplication, triplication | A30P: late onset, L-dopa responded parkinsonism; A53T: typical parkinsonism with rapid progression; E64K: DLB-like symptoms; duplication: typical parkinsonism; triplication: early onset parkinsonism with rapid progression |
| PARK2 | AR | PRKN | Nonsense, frameshift, missense | Early onset, symmetric, slowly progressed parkinsonism with spasticity and sleep benefits |
| PARK3 | AD | Unknown | – | – |
| PARK5 | AD | UCH-L1 | Missense | Similar to sporadic PD |
| PARK6 | AR | PINK1 | Nonsense, frameshift, missense | Early onset typical parkinsonism with psychiatric symptoms and L-dopa associated dyskinesia |
| PARK7 | AR | DJ-1 | Missense | Early onset parkinsonism with psychiatric symptoms, occasionally with scoliosis and blephalospasm |
| PARK8 | AD | LRRK2 | Missense | Middle to late onset typical parkinsonism with response to L-dopa |
| PARK9 | AR | ATP13A2 | Missense, deletion, insertion, duplication | Rapidly progressed parkinsonism with dementia and pyramidal features |
| PARK10 | Sporadic | Unknown | – | – |
| PARK11 | AD | Unknown | – | – |
| PARK12 | Sporadic | Unknown | – | – |
| PARK13 | AD | Omi/HtrA2 | Missense | Typical parkinsonism |
| PARK14 | AR | PLA2G6 | Missense | Early onset parkinsonism with rapid progression, cognitive decline and brain atrophy (cerebellum and cerebrum) |
| PARK15 | AR | FBXO7 | Missense, frameshift | Early onset parkinsonism with spasticity and response to L-dopa |
| PARK16 | Sporadic | Unknown | – | – |

AD, autosomal dominant; AR, autosomal recessive; DLB, dementia with Lewy bodies; PD, Parkinson's disease.

dependent manner by restricting conformational fluctuations of α-synuclein.[16] Recent advances in research on the protein degradation system associated with PD revealed the importance of ubiquitin proteasome and the autophagy–lysosome pathway in disease pathogenesis.[17] Wild-type α-synuclein is degraded by both chaperone mediated autophagy and macroautophagy, while A30P and A53T are degraded mainly by the latter.[17–19] Furthermore, macroautophagy itself is blocked by α-synuclein via Rap1a dysregulation.[20]

Several lines of evidence have shown that permeabilised α-synuclein from a neuron may be toxic to neurons and/or glias they are next to. Actually, grafted healthy neurons can gradually develop the same pathology as host neurons in PD brains.[21] These findings have suggested that non-cell autonomous cell death as well as cell autonomous cell death may have an important role in disease pathogenesis.

## Parkin (PARK2)

### Clinicogenetics

The first genetic locus for autosomal recessive juvenile parkinsonism was mapped to chromosome 6, and the disease gene named parkin (*PRKN*) was identified in consanguineous families.[22–24] Mutations in the *PRKN* gene are most common in autosomal recessive juvenile parkinsonism and many mutations have been reported.[3] The clinical picture is similar to that of sPD except for earlier onset, dystonic features, brisk reflexes and sleep benefit. Pathologically, no Lewy bodies were seen in most cases.[25–27] Whether or not heterozygous *PRKN* mutations may cause or increase the susceptibility to late onset typical PD remains controversial. [18F]Fluorodopa uptake by positron emission tomography was reduced in heterozygous carriers without symptoms.[28 29] In addition, heterozygous carriers of *PRKN* mutations have been reported to have either minor motor signs or present with late onset parkinsonism, suggesting a link between heterozygous mutations and disease pathogenesis.[27 30 31] On the other hand, screening for *PRKN* mutations in late onset PD and healthy controls revealed similar frequencies of genetic variants.[32 33]

### Molecular biology

Parkin is associated with the ubiquitin proteasome system as an E3 ubiquitin ligase.[34] The C terminal binds with ubiquitin E2 enzymes and recognises a substrate whereas the N terminal interacts with the 19S subunit of proteasome. A nonsense mutation lacking the rear RING finger motif had no E3 activity and sole IBR-RING2 retained E3 activity, and thus most parkin mutations do not lead to loss of kinase activity.[35] α-Synuclein and synphilin-1 were identified as parkin substrates and consist of Lewy bodies.[36 37] Parkin mainly localises in the cytoplasm as well as in plasma membranes and partly in mitochondria. Under physiological or pathological conditions, parkin is involved in mitochondrial maintenance and recent evidence revealed that parkin with PINK1 physically associate and functionally cooperate to identify and label damaged mitochondria for selective degradation via autophagy (mitophagy).[38–42] Protein–protein interactions between parkin and other PD related genes are detailed in each gene section.

## PINK1 (PARK6)

### Clinicogenetics

PARK6 was first identified on chromosome 1p36.[43] The disease gene was identified as *PINK1* (PTEN induced kinase 1) containing eight exons.[44] The clinical characteristics are autosomal recessive, early onset, slow disease progression and L-dopa responsive parkinsonism. Most mutations were missense mutations, but whole gene deletions were also reported.[45 46] Many putative pathogenic mutations were also observed in a heterozygous state in familial and sPD patients as well as in healthy controls. However, most of the studies have not checked the copy number variants, causing the mutation pathogenicity to remain controversial.[2] Lewy bodies, neuronal loss and astrocytic gliosis in the substantia nigra were detected in a patient with *PINK1* compound heterozygous mutations.[47]

### Molecular biology

PINK1 has eight exons encoding 581 amino acids, including a mitochondrial targeting sequence, transmembrane domain and



Saiki S, Sato S, Hattori N. *J Neurol Neurosurg Psychiatry* (2011). doi:10.1136/jnnp-2011-301205

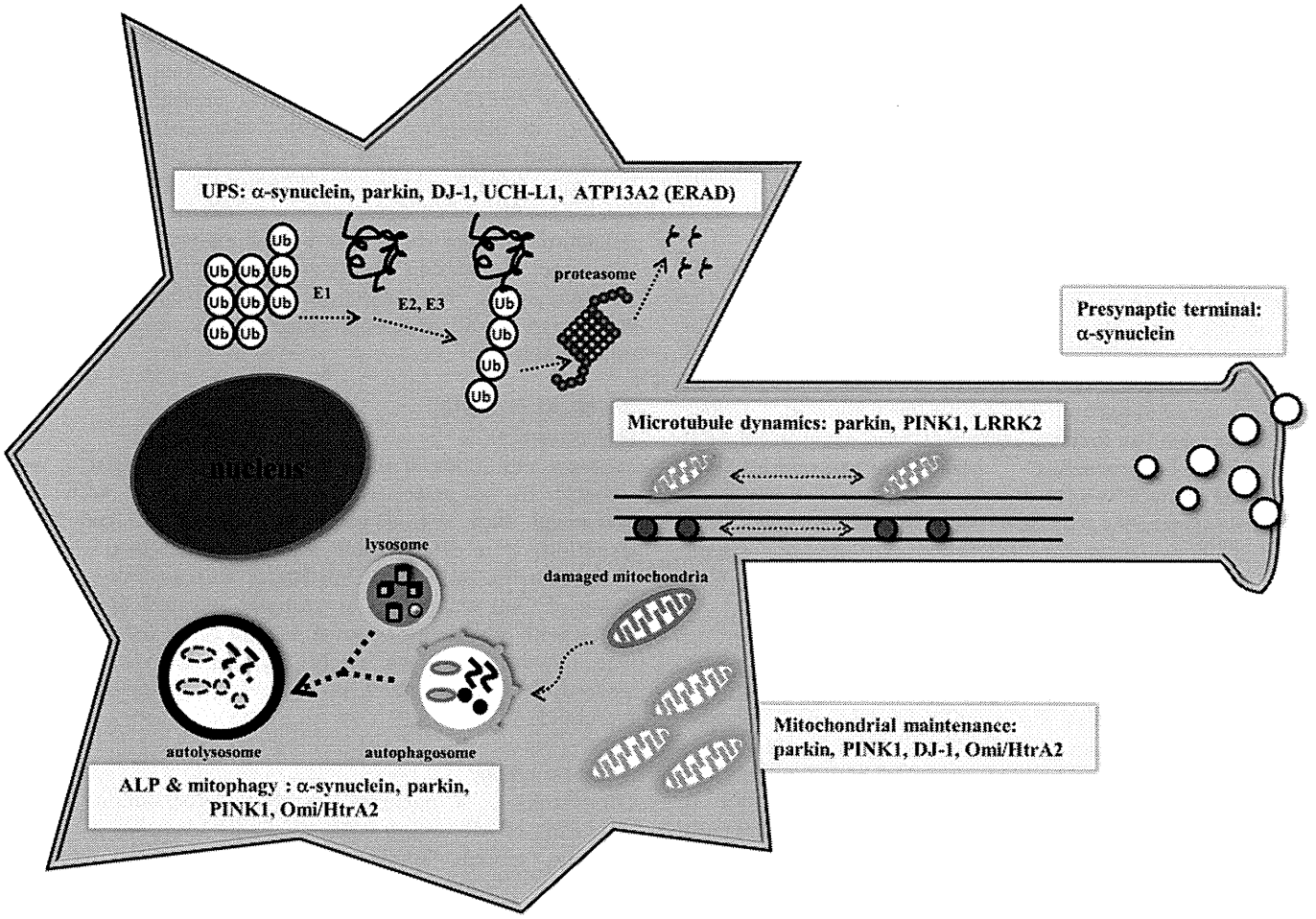


**Figure 1** Schematic representation of the possible pathogenesis in hereditary Parkinson's disease. ALP, autophagy—lysosome pathway; ERAD, endoplasmic reticulum associated degradation; Ub, ubiquitin; UPS, ubiquitin proteasome system.

kinase domain.[48] The gene product is ubiquitously expressed in the brain and systemic organs. The protein mainly localises in mitochondria, especially in the outer membrane. PINK1 is a serine—threonine kinase and several pathological mutations in PINK1 have been reported to change their kinase activities.[49–52] In addition, Rictor (a component of mTORC2),[53] tumour necrosis factor receptor associated protein 1 (TRAP1; a mitochondrial chaperone),[50] Omi (PARK13 gene product) and parkin (PARK2 gene product) were identified as substrates for PINK1.[54 55]

PINK1 regulates mitochondrial dynamics and respiratory functions.[38 53 56–58] Mitochondrial fission is accelerated by PINK1 overexpression accompanied by parkin.[59 60] PINK1 ablation with siRNA in neurons reduces resistance against oxidative stress while its overexpression provides resistance.[61] Using genetically modified Drosophila models, we see that PINK1 deficiency causes the same phenotype as parkin deficiency and the PINK1 deficiency phenotype is rescued by parkin complementation, suggesting that parkin is downstream of PINK1.[62–64] Several lines of evidence have provided new aspects of the PINK1/parkin pathway associated with mitochondrial elimination via macroautophagy (mitophagy). When mitochondrial membrane potentials are lost, endogenous PINK1 is accumulated followed by parkin recruitment, and subsequently the depolarised mitochondria were eliminated by mitophagy.[40 41 65 66] Mitochondrial targeting sequence, kinase activity of PINK1 and the linker domain of parkin are indispensable for the PINK1/parkin mediated mitophagy.

## DJ-1 (PARK7)

### Clinicogenetics

Clinical features of *PARK7* are characterised by early onset parkinsonism with scoliosis, blephalospasm and psychiatric symptoms, similar to those of *PARK2* and *PARK6*. The disease gene was identified as *DJ-1*, which has eight exons encoding 189 amino acids. Three missense mutations (L166P, M26I, E64D) in exons 1–5 of the gene have been identified in Italian, Dutch and Uruguayan families. *DJ-1* protein was detected around Lewy bodies, suggesting *DJ-1* is not in the main structure of Lewy bodies. However, the protein was detected in astrocytes and in a part of the cytoplasmic inclusions positive to tau in brains with corticobasal degeneration, progressive supranuclear palsy and multiple system atrophy.[67–69]

### Molecular biology

DJ-1 is almost ubiquitously expressed in organs, including the brain. Endogenous DJ-1 is present in synaptic terminals, mitochondria and membranous organelles.[70 71] DJ-1 with the L166P mutation lost more stability compared with the wild-type and mutant DJ-1 (M26I, E64D).[72] In DJ-1 knockout mice, no significant loss of dopaminergic neurons and decreased susceptibility to oxidative stress were noted.[73] DJ-1 is a multifunctional redox sensitive protein regulating mitochondrial oxidative stress and increases expression levels of SOD1 in an Erk1/2-Elk1 pathway dependent manner,[74] and facilitates prosurvival factor Akt, leading to suppression of apoptosis.[75] Also, the protein

inhibits TRAIL induced apoptosis by blocking Fas associated protein death domain mediated pro-caspase-8 activation.[76] Along with parkin and PINK1, DJ-1 has various cellular functions such as regulation of mitochondrial morphology as well as misfolded protein degradation by forming an E3 ligase complex with those proteins.[77]

## LRRK2 (PARK8)

### Clinicogenetics

Clinical features of PARK8 are essentially similar to those of sPD except for earlier onset age. The disease gene was identified as the leucine rich repeat kinase 2 gene (*LRRK2*) linked to autosomal dominant inherited PD encoding 2517 amino acids.[78–80] PARK8 is the most common form of hPD in the world. Until now, 20 missense or nonsense mutations have been reported.[81] *LRRK2* mutations were also found in some sPD cases; neuropathological findings were heterogeneous.[82 83] Most of the cases with *LRRK2* mutations showed various degrees of Lewy bodies but intraneuronal aggregations positive to tau were rarely detected.[79 84 85] The G2019S mutation in *LRRK2* is the most common genetic cause of PD, accounting for a significant proportion of both autosomal dominant and sPD cases.

### Molecular biology

LRRK2 protein, containing a GTPase domain, a Ras of complex domain, a C terminal of Ras complex domain and a mitogen activated kinase domain, is highly expressed in the brain, and mRNA levels are rich in the striatum and hippocampus compared with other regions.[86] Intracellular LRRK2 is mainly distributed in the plasma membrane and vesicular structures.[87 88] Immunoprecipitation techniques have revealed that LRRK2 interacts with parkin.[89] In transgenic flies, neurodegeneration by LRRK2 with or without a mutation is modified by overexpression or siRNA knockdown of parkin, PINK1 or DJ-1, suggesting genetic interaction between them.[90 91] Activity changes of LRRK2 kinase and GTPase have been suspected as a key factor in LRRK pathogenesis. Changes in LRRK2 activity cause alterations in mitogen activated protein kinase, translational control, tumour necrosis factor α/Fas ligand and Wnt signalling pathways with the cell biological functions of LRRK2 such as vesicle trafficking.[80] The most common pathological mutation in LRRK2, G2019S LRRK2, causes neurite retraction by activation of Rac1 small GTPase.[92] LRRK2 mutations inhibit an endogenous peroxidase by phosphorylation promoting dysregulation of mitochondrial function and oxidative damage.[93] G2019S human LRRK2 transgenic rat models specifically expressed in the nigrostriatal system have shown progressive degeneration of nigral dopaminergic neurons.[94] In terms of LRRK2 control, PKA has been identified as a potential upstream kinase of LRRK2 at S935, on which binding of 14-3-3 with LRRK2 depends.[95] However, the exact biological function of LRRK2 remains largely unclear because no physiological substrates have been identified to date.

## ATP13A2 (PARK9)

### Clinicogenetics

PARK9, also known as Kufor–Rakeb syndrome, is an autosomal recessive parkinsonian disorder characterised by early onset (14–16 years old), good response to L-dopa treatment, pyramidal feature, supranuclear gaze palsy and dementia.[96] The gene locus was mapped to 1p36 and the disease gene was identified as *ATP13A2*, which localises in lysosomal membranes.[97] Various types of mutations in the *ATP13A2* have been reported.

### Molecular biology

ATP13A2 is predicted to be a lysosomal P5-type ATPase that plays important roles in regulating cation homeostasis. Although ATP13A2 function remains unclear, it might be involved in protecting cells against manganese and mutant α-synuclein toxicity.[98] Wild-type ATP13A2 localises mainly in lysosomes whereas three separate mutants with a mutation involved in PD cause retention of the protein in the endoplasmic reticulum, and are eliminated by the endoplasmic reticulum associated degradation pathway.[99] Wild-type ATP13A2, but not pathogenic mutants, reduced intracellular manganese concentration and prevented cytochrome C release from the mitochondria.[100]

## Omi/HtrA2 (PARK13)

### Clinicogenetics

Missense mutations in the gene coding for Omi/HtrA2 were reported to be associated with four patients with sPD, presenting with typical parkinsonism.[55] G399S and A141S mutations were detected and resulted in defective activation of the protease activity of Omi/HtrA2. Pathologically, accumulation of Omi was found in neuronal and glial inclusions in brains with α-synucleinopathies as well as in Lewy bodies.[101] The largest association study revealed no overall strong association of Omi/HtrA2 variants with sPD in populations worldwide.[102]

### Molecular biology

Omi/HtrA2 is a nuclearly encoded mitochondrial protein consisting of 458 amino acids, originally identified as a proapoptotic protein binding with an apoptosis inhibiting protein.[103 104] Omi knockout mice presented with neuronal loss in the striatum and died within 30 days of birth.[105] Cells overexpressing Omi mutant with G399S have shown mitochondrial morphological changes followed by dysfunction and increased susceptibility against oxidative stress.[55] Interestingly, wild-type Omi/HtrA2, not protease defective mutant, activates autophagy through digestion of Hax-1, a Bcl-2 family related protein that represses autophagy via Beclin-1 inhibition, suggesting an insufficient protein degradation system may play a key role.[106]

## PLA2G6 (PARK14)

### Clinicogenetics

PARK14 is an autosomal recessive parkinsonian syndrome characterised by early onset rapidly progressive parkinsonism, dystonia, cognitive decline, and cerebral and cerebellar atrophy. Through homozygosity mapping and direct sequencing, two different homozygous mutations in *PLA2G6*, which also causes infantile neuroaxonal dystrophy and neurodegeneration with brain iron accumulation, were identified.[107 108] Cranial MRI did not detect iron accumulation in the basal ganglia in most cases with this disorder.[108 109]

### Molecular biology

The PLA2G6 gene encodes a group VIA calcium independent phospholipase A2, also known as calcium independent phospholipase A2 β, which hydrolyses the sn-2 acyl chain of phospholipids, generating free fatty acids and lysophospholipids. In an in vitro assay, wild-type PLA2G6 associated with infantile neuroaxonal dystrophy/neurodegeneration with brain iron accumulation failed to catalyse fatty acid release from phospholipids, while PARK14 associated mutations ((R741Q, R747W and R632W) did not, implying that other functions of PLA2G6



Saiki S, Sato S, Hattori N. *J Neurol Neurosurg Psychiatry* (2011). doi:10.1136/jnnp-2011-301205

include interactions with calmodulin and that PLA2G6 might also be associated with calcium/calmodulin dependent protein kinase II-β.[110 111]

## FBXO7 (PARK15)

### Clinicogenetics

Only three families with mutations in *FBXO7* have been reported.[112 113] Affected individuals had juvenile onset (10–19 years old) of progressive parkinsonism associated with spasticity, and variable response to L-dopa. No pathological studies have been reported.

### *Molecular biology*

Fbox7 is a member of the F box containing protein (FBP) family with an F box domain. F box containing proteins are expected to function as molecular scaffolds in the formation of the protein complex; however, the exact function of FBXO7 remains unclear.

## OTHER GENES ASSOCIATED WITH PARKINSON'S DISEASE

GWAS have uncovered a number of candidate genes involved in PD in European and Japanese populations, indicating a substantial contribution of genetics underlying susceptibility to both early onset and late onset PD.[6 7 114–119] These studies have shown repeatedly a common variation in *SNCA* and an inversion of the region containing the *MAPT*. Recent genetic studies revealed mutations in the *GBA* gene, the most widespread genetic risk factor for parkinsonism identified to date.[120–124] In this section, we summarise the molecular mechanisms of the two genes, MAPT and GBA.

## MAPT

Mutations in *MAPT*, encoding microtubule associated tau, result in tauopathies, including progressive supuranuclear palsy, corticobasal degeneration and frontotemporal lobar degeneration.[125] Tau is a soluble protein, but insoluble aggregates are produced during the formation of neurofibrillary tangles which disrupts microtubule associated dynamics and neuronal functions. Considering the interplay between α-synuclein and tau reported previously,[126] it is interesting that there would be a common pathogenesis associated with aggregation formations.

## GBA

Early observed patients with Gaucher disease and their heterozygous relatives present with parkinsonism.[127] In addition, autopsy studies have shown the presence of mutant glucocerebrosidase (GCase) in α-synuclein positive Lewy bodies in Gaucher disease patients and carriers with α-synucleinopathies.[128] GCase is a lysosomal hydrolase with 497 amino acids that catalyses the metabolism of the glycolipid glucosylceramide to ceramide and glucose. Cells overexpressing mutant GCase promoted α-synuclein accumulation in a dose and time dependent manner.[129] α-Synuclein GCase interacts selectively under lysosomal solution conditions (pH 5.5) and the interaction site was mapped to the α-synuclein C terminal residues 118–137.[130] Insufficient functions of the lysosomes may have an effect on chaperone mediated autophagy or macroautophagy.

## CONCLUDING REMARKS

In the 14 years since the first causative gene (α-synuclein) in PD was discovered, great advances have been made in understanding the biology of the disease. Recent evidence shows that the environment plays no role in the aetiology of PD.[131] In addition, GWAS suggest that a number of genes influence susceptibility.[3] The PD associated genes provide valuable clues regarding the molecular pathogenesis of PD because the pathomechanism for sPD would have certain pathways in common with those of hPD. Importantly, basic biological studies in PD have led to numerous potential therapeutic strategies. For example, a specific inhibitor for LRRK2 phosphorylations at Ser910 and Ser935 was recently developed.[132] In the future, it becomes more important to translate laboratory data, including molecular pathogenesis as well as genetic associations, into clinical treatments, leading to disease modifying therapies to conquer the disease onset and/or progression.

**Funding** The authors are very grateful for the CREST Grant from the Japan Science and Technology Agency (NH), grants from the Ministry of Health, Labour and Welfare (NH) and the Ministry of Education, Culture, Sports, Science and Technology (NH), Grant-in-Aid for Young Scientists (A) (S Saiki), a promoted grant from Juntendo University (S Saiki) and grants from the Takeda Scientific Foundation (S Sato, S Saiki) and the Life Science Foundation (S Saiki).

**Competing interests** None.

**Contributors** All authors contributed to this work, including interpretation of the references and manuscript writing.

**Provenance and peer review** Commissioned; externally peer reviewed.

## REFERENCES

1. **Hatano T,** Kubo S, Sato S, *et al*. Pathogenesis of familial Parkinson's disease: new insights based on monogenic forms of Parkinson's disease. *J Neurochem* 2009;**111**:1075–93.
2. **Nuytemans K,** Theuns J, Cruts M, *et al*. Genetic etiology of Parkinson disease associated with mutations in the SNCA, PARK2, PINK1, PARK7, and LRRK2 genes: a mutation update. *Hum Mutat* 2010;**31**:763–80.
3. **Gasser T.** Molecular pathogenesis of Parkinson disease: insights from genetic studies. *Expert Rev Mol Med* 2009;**11**:e22.
4. **Polymeropoulos MH,** Lavedan C, Leroy E, *et al*. Mutation in the alpha-synuclein gene identified in families with Parkinson's disease. *Science* 1997;**276**:2045–7.
5. **Venda LL,** Cragg SJ, Buchman VL, *et al*. α-Synuclein and dopamine at the crossroads of Parkinson's disease. *Trends Neurosci* 2010;**33**:559–68.
6. **Simon-Sanchez J,** Schulte C, Bras JM, *et al*. Genome-wide association study reveals genetic risk underlying Parkinson's disease. *Nat Genet* 2009;**41**:1308–12.
7. **Satake W,** Nakabayashi Y, Mizuta I, *et al*. Genome-wide association study identifies common variants at four loci as genetic risk factors for Parkinson's disease. *Nat Genet* 2009;**41**:1303–7.
8. **Farrer M,** Maraganore DM, Lockhart P, *et al*. α-Synuclein gene haplotypes are associated with Parkinson's disease. *Hum Mol Genet* 2001;**10**:1847–51.
9. **Maraganore DM,** de Andrade M, Elbaz A, *et al*. Collaborative analysis of alpha-synuclein gene promoter variability and Parkinson disease. *JAMA* 2006;**296**:661–70.
10. **Giasson BI,** Duda JE, Murray IV, *et al*. Oxidative damage linked to neurodegeneration by selective alpha-synuclein nitration in synucleinopathy lesions. *Science* 2000;**290**:985–9.
11. **Kruger R,** Eberhardt O, Riess O, *et al*. Parkinson's disease: one biochemical pathway to fit all genes? *Trends Mol Med* 2002;**8**:236–40.
12. **Masliah E,** Rockenstein E, Veinbergs I, *et al*. Dopaminergic loss and inclusion body formation in alpha-synuclein mice: implications for neurodegenerative disorders. *Science* 2000;**287**:1265–9.
13. **Kahle PJ,** Neumann M, Ozmen L, *et al*. Subcellular localization of wild-type and Parkinson's disease-associated mutant alpha-synuclein in human and transgenic mouse brain. *J Neurosci* 2000;**20**:6365–73.
14. **Giasson BI,** Duda JE, Quinn SM, *et al*. Neuronal alpha-synucleinopathy with severe movement disorder in mice expressing A53T human alpha-synuclein. *Neuron* 2002;**34**:521–33.
15. **Cookson MR,** van der Brug M. Cell systems and the toxic mechanism(s) of alpha-synuclein. *Exp Neurol* 2008;**209**:5–11.
16. **Falsone SF,** Kungl AJ, Rek A, *et al*. The molecular chaperone Hsp90 modulates intermediate steps of amyloid assembly of the Parkinson-related protein alpha-synuclein. *J Biol Chem* 2009;**284**:31190–9.
17. **Webb JL,** Ravikumar B, Atkins J, *et al*. Alpha-synuclein is degraded by both autophagy and the proteasome. *J Biol Chem* 2003;**278**:25009–13.
18. **Cuervo AM,** Stefanis L, Fredenburg R, *et al*. Impaired degradation of mutant alpha-synuclein by chaperone-mediated autophagy. *Science* 2004;**305**:1292–5.
19. **Martinez-Vicente M,** Talloczy Z, Kaushik S, *et al*. Dopamine-modified alpha-synuclein blocks chaperone-mediated autophagy. *J Clin Invest* 2008;**118**:777–88.
20. **Winslow AR,** Chen CW, Corrochano S, *et al*. α-Synuclein impairs macroautophagy: implications for Parkinson's disease. *J Cell Biol* 2010;**190**:1023–37.
21. **Brundin P,** Li JY, Holton JL, *et al*. Research in motion: the enigma of Parkinson's disease pathology spread. *Nat Rev Neurosci* 2008;**9**:741–5.

22. **Kitada T,** Asakawa S, Hattori N, *et al*. Mutations in the parkin gene cause autosomal recessive juvenile parkinsonism. *Nature* 1998;**392**:605—8.
23. **Hattori N,** Kitada T, Matsumine H, *et al*. Molecular genetic analysis of a novel parkin gene in Japanese families with autosomal recessive juvenile parkinsonism: evidence for variable homozygous deletions in the parkin gene in affected individuals. *Ann Neurol* 1998;**44**:935—41.
24. **Matsumine H,** Saito M, Shimoda-Matsubayashi S, *et al*. Localization of a gene for an autosomal recessive form of juvenile Parkinsonism to chromosome 6q25.2-27. *Am J Hum Genet* 1997;**60**:588—96.
25. **Mori H,** Kondo T, Yokochi M, *et al*. Pathologic and biochemical studies of juvenile parkinsonism linked to chromosome 6q. *Neurology* 1998;**51**:890—2.
26. **Takahashi H,** Ohama E, Suzuki S, *et al*. Familial juvenile parkinsonism: clinical and pathologic study in a family. *Neurology* 1994;**44**:437—41.
27. **Farrer M,** Chan P, Chen R, *et al*. Lewy bodies and parkinsonism in families with parkin mutations. *Ann Neurol* 2001;**50**:293—300.
28. **Hilker R,** Klein C, Ghaemi M, *et al*. Positron emission tomographic analysis of the nigrostriatal dopaminergic system in familial parkinsonism associated with mutations in the parkin gene. *Ann Neurol* 2001;**49**:367—76.
29. **Khan NL,** Brooks DJ, Pavese N, *et al*. Progression of nigrostriatal dysfunction in a parkin kindred: an [18F]dopa PET and clinical study. *Brain* 2002;**125**:2248—56.
30. **Klein C,** Pramstaller PP, Kis B, *et al*. Parkin deletions in a family with adult-onset, tremor-dominant parkinsonism: expanding the phenotype. *Ann Neurol* 2000;**48**:65—71.
31. **Pramstaller PP,** Kis B, Eskelson C, *et al*. Phenotypic variability in a large kindred (Family LA) with deletions in the parkin gene. *Mov Disord* 2002;**17**:424—6.
32. **Lincoln SJ,** Maraganore DM, Lesnick TG, *et al*. Parkin variants in North American Parkinson's disease: cases and controls. *Mov Disord* 2003;**18**:1306—11.
33. **Kay DM,** Moran D, Moses L, *et al*. Heterozygous parkin point mutations are as common in control subjects as in Parkinson's patients. *Ann Neurol* 2007;**61**:47—54.
34. **Shimura H,** Hattori N, Kubo S, *et al*. Familial Parkinson disease gene product, parkin, is a ubiquitin-protein ligase. *Nat Genet* 2000;**25**:302—5.
35. **Matsuda N,** Kitami T, Suzuki T, *et al*. Diverse effects of pathogenic mutations of Parkin that catalyze multiple monoubiquitylation in vitro. *J Biol Chem* 2006;**281**:3204—9.
36. **Shimura H,** Schlossmacher MG, Hattori N, *et al*. Ubiquitination of a new form of alpha-synuclein by parkin from human brain: implications for Parkinson's disease. *Science* 2001;**293**:263—9.
37. **Chung KK,** Zhang Y, Lim KL, *et al*. Parkin ubiquitinates the alpha-synuclein-interacting protein, synphilin-1: implications for Lewy-body formation in Parkinson disease. *Nat Med* 2001;**7**:1144—50.
38. **Weihofen A,** Thomas KJ, Ostaszewski BL, *et al*. Pink1 forms a multiprotein complex with Miro and Milton, linking Pink1 function to mitochondrial trafficking (dagger). *Biochemistry* 2009;**48**:2045—52.
39. **Narendra D,** Tanaka A, Suen DF, *et al*. Parkin is recruited selectively to impaired mitochondria and promotes their autophagy. *J Cell Biol* 2008;**183**:795—803.
40. **Narendra D,** Kane LA, Hauser DN, *et al*. p62/SQSTM1 is required for Parkin-induced mitochondrial clustering but not mitophagy; VDAC1 is dispensable for both. *Autophagy* 2010;**6**:1090—106.
41. **Matsuda N,** Sato S, Shiba K, *et al*. PINK1 stabilized by mitochondrial depolarization recruits Parkin to damaged mitochondria and activates latent Parkin for mitophagy. *J Cell Biol* 2010;**189**:211—21.
42. **Park J,** Lee G, Chung J. The PINK1—Parkin pathway is involved in the regulation of mitochondrial remodeling process. *Biochem Biophys Res Commun* 2009;**378**:518—23.
43. **Valente EM,** Bentivoglio AR, Dixon PH, *et al*. Localization of a novel locus for autosomal recessive early-onset parkinsonism, PARK6, on human chromosome 1p35-p36. *Am J Hum Genet* 2001;**68**:895—900.
44. **Valente EM,** Abou-Sleiman PM, Caputo V, *et al*. Hereditary early-onset Parkinson's disease caused by mutations in PINK1. *Science* 2004;**304**:1158—60.
45. **Marongiu R,** Brancati F, Antonini A, *et al*. Whole gene deletion and splicing mutations expand the PINK1 genotypic spectrum. *Hum Mutat* 2007;**28**:98.
46. **Hatano Y,** Li Y, Sato K, *et al*. Novel PINK1 mutations in early-onset parkinsonism. *Ann Neurol* 2004;**56**:424—7.
47. **Samaranch L,** Lorenzo-Betancor O, Arbelo JM, *et al*. PINK1-linked parkinsonism is associated with Lewy body pathology. *Brain* 2010;**133**:1128—42.
48. **Kawajiri S,** Saiki S, Sato S, *et al*. Genetic mutations and functions of PINK1. *Trends Pharmacol Sci* 2011;**32**:573—80.
49. **Beilina A,** Van Der Brug M, Ahmad R, *et al*. Mutations in PTEN-induced putative kinase 1 associated with recessive parkinsonism have differential effects on protein stability. *Proc Natl Acad Sci U S A* 2005;**102**:5703—8.
50. **Pridgeon JW,** Olzmann JA, Chin LS, *et al*. PINK1 protects against oxidative stress by phosphorylating mitochondrial chaperone TRAP1. *PLoS Biol* 2007;**5**:e172.
51. **Silvestri L,** Caputo V, Bellacchio E, *et al*. Mitochondrial import and enzymatic activity of PINK1 mutants associated to recessive parkinsonism. *Hum Mol Genet* 2005;**14**:3477—92.
52. **Sim CH,** Lio DS, Mok SS, *et al*. C-terminal truncation and Parkinson's disease-associated mutations down-regulate the protein serine/threonine kinase activity of PTEN-induced kinase-1. *Hum Mol Genet* 2006;**15**:3251—62.
53. **Murata H,** Sakaguchi M, Jin Y, *et al*. A new cytosolic pathway from a Parkinson disease-associated kinase, BRPK/PINK1: activation of AKT via mTORC2. *J Biol Chem* 2011;**286**:7182—9.
54. **Plun-Favreau H,** Klupsch K, Moisoi N, *et al*. The mitochondrial protease HtrA2 is regulated by Parkinson's disease-associated kinase PINK1. *Nat Cell Biol* 2007;**9**:1243—52.
55. **Strauss KM,** Martins LM, Plun-Favreau H, *et al*. Loss of function mutations in the gene encoding Omi/HtrA2 in Parkinson's disease. *Hum Mol Genet* 2005;**14**:2099—111.
56. **Wang X,** Schwarz TL. The mechanism of Ca2+ -dependent regulation of kinesin-mediated mitochondrial motility. *Cell* 2009;**136**:163—74.
57. **Liu W,** Vives-Bauza C, Acin-Perez R, *et al*. PINK1 defect causes mitochondrial dysfunction, proteasomal deficit and alpha-synuclein aggregation in cell culture models of Parkinson's disease. *PLoS One* 2009;**4**:e4597.
58. **Amo T,** Sato S, Saiki S, *et al*. Mitochondrial membrane potential decrease caused by loss of PINK1 is not due to proton leak, but to respiratory chain defects. *Neurobiol Dis* 2011;**41**:111—8.
59. **Deng H,** Dodson MW, Huang H, *et al*. The Parkinson's disease genes pink1 and parkin promote mitochondrial fission and/or inhibit fusion in Drosophila. *Proc Natl Acad Sci U S A* 2008;**105**:14503—8.
60. **Poole AC,** Thomas RE, Andrews LA, *et al*. The PINK1/Parkin pathway regulates mitochondrial morphology. *Proc Natl Acad Sci U S A* 2008;**105**:1638—43.
61. **Haque ME,** Thomas KJ, D'Souza C, *et al*. Cytoplasmic Pink1 activity protects neurons from dopaminergic neurotoxin MPTP. *Proc Natl Acad Sci U S A* 2008;**105**:1716—21.
62. **Clark IE,** Dodson MW, Jiang C, *et al*. Drosophila pink1 is required for mitochondrial function and interacts genetically with parkin. *Nature* 2006;**441**:1162—6.
63. **Park J,** Lee SB, Lee S, *et al*. Mitochondrial dysfunction in Drosophila PINK1 mutants is complemented by parkin. *Nature* 2006;**441**:1157—61.
64. **Yang Y,** Gehrke S, Imai Y, *et al*. Mitochondrial pathology and muscle and dopaminergic neuron degeneration caused by inactivation of Drosophila Pink1 is rescued by Parkin. *Proc Natl Acad Sci U S A* 2006;**103**:10793—8.
65. **Kawajiri S,** Saiki S, Sato S, *et al*. PINK1 is recruited to mitochondria with parkin and associates with LC3 in mitophagy. *FEBS Lett* 2010;**584**:1073—9.
66. **Youle RJ,** Narendra DP. Mechanisms of mitophagy. *Nat Rev Mol Cell Biol* 2011;**12**:9—14.
67. **Abou-Sleiman PM,** Healy DG, Quinn N, *et al*. The role of pathogenic DJ-1 mutations in Parkinson's disease. *Ann Neurol* 2003;**54**:283—6.
68. **Bandopadhyay R,** Kingsbury AE, Cookson MR, *et al*. The expression of DJ-1 (PARK7) in normal human CNS and idiopathic Parkinson's disease. *Brain* 2004;**127**:420—30.
69. **Neumann M,** Muller V, Gorner K, *et al*. Pathological properties of the Parkinson's disease-associated protein DJ-1 in alpha-synucleinopathies and tauopathies: relevance for multiple system atrophy and Pick's disease. *Acta Neuropathol* 2004;**107**:489—96.
70. **Olzmann JA,** Bordelon JR, Muly EC, *et al*. Selective enrichment of DJ-1 protein in primate striatal neuronal processes: implications for Parkinson's disease. *J Comp Neurol* 2007;**500**:585—99.
71. **Usami Y,** Hatano T, Imai S, *et al*. DJ-1 associates with synaptic membranes. *Neurobiol Dis* 2011;**43**:651—62.
72. **Miller DW,** Ahmad R, Hague S, *et al*. L166P mutant DJ-1, causative for recessive Parkinson's disease, is degraded through the ubiquitin-proteasome system. *J Biol Chem* 2003;**278**:36588—95.
73. **Goldberg MS,** Pisani A, Haburcak M, *et al*. Nigrostriatal dopaminergic deficits and hypokinesia caused by inactivation of the familial parkinsonism-linked gene DJ-1. *Neuron* 2005;**45**:489—96.
74. **Wang Z,** Liu J, Chen S, *et al*. DJ-1 modulates the expression of Cu/Zn-superoxide dismutase-1 through the Erk1/2-Elk1 pathway in neuroprotection. *Ann Neurol* 2011;**70**:591—9.
75. **Lev N,** Roncevic D, Ickowicz D, *et al*. Role of DJ-1 in Parkinson's disease. *J Mol Neurosci* 2006;**29**:215—25.
76. **Fu K,** Ren H, Wang Y, *et al*. DJ-1 inhibits TRAIL-induced apoptosis by blocking pro-caspase-8 recruitment to FADD. *Oncogene*. Published Online First: 25 July 2011. doi:10.1038/onc.2011.315.
77. **Xiong H,** Wang D, Chen L, *et al*. Parkin, PINK1, and DJ-1 form a ubiquitin E3 ligase complex promoting unfolded protein degradation. *J Clin Invest* 2009;**119**:650—60.
78. **Paisan-Ruiz C,** Jain S, Evans EW, *et al*. Cloning of the gene containing mutations that cause PARK8-linked Parkinson's disease. *Neuron* 2004;**44**:595—600.
79. **Zimprich A,** Biskup S, Leitner P, *et al*. Mutations in LRRK2 cause autosomal-dominant parkinsonism with pleomorphic pathology. *Neuron* 2004;**44**:601—7.
80. **Berwick DC,** Harvey K. LRRK2 signaling pathways: the key to unlocking neurodegeneration? *Trends Cell Biol* 2011;**21**:257—65.
81. **Cookson MR.** The role of leucine-rich repeat kinase 2 (LRRK2) in Parkinson's disease. *Nat Rev Neurosci* 2010;**11**:791—7.
82. **Gilks WP,** Abou-Sleiman PM, Gandhi S, *et al*. A common LRRK2 mutation in idiopathic Parkinson's disease. *Lancet* 2005;**365**:415—16.
83. **Wszolek ZK,** Pfeiffer RF, Tsuboi Y, *et al*. Autosomal dominant parkinsonism associated with variable synuclein and tau pathology. *Neurology* 2004;**62**:1619—22.
84. **Ross OA,** Toft M, Whittle AJ, *et al*. Lrrk2 and Lewy body disease. *Ann Neurol* 2006;**59**:388—93.
85. **Dachsel JC,** Ross OA, Mata IF, *et al*. Lrrk2 G2019S substitution in frontotemporal lobar degeneration with ubiquitin-immunoreactive neuronal inclusions. *Acta Neuropathol* 2007;**113**:601—6.

86. **Galter D,** Westerlund M, Carmine A, *et al*. LRRK2 expression linked to dopamine-innervated areas. *Ann Neurol* 2006;**59**:714–19.
87. **Hatano T,** Kubo S, Imai S, *et al*. Leucine-rich repeat kinase 2 associates with lipid rafts. *Hum Mol Genet* 2007;**16**:678–90.
88. **Biskup S,** Moore DJ, Celsi F, *et al*. Localization of LRRK2 to membranous and vesicular structures in mammalian brain. *Ann Neurol* 2006;**60**:557–69.
89. **Smith WW,** Pei Z, Jiang H, *et al*. Leucine-rich repeat kinase 2 (LRRK2) interacts with parkin, and mutant LRRK2 induces neuronal degeneration. *Proc Natl Acad Sci U S A* 2005;**102**:18676–81.
90. **Ng CH,** Mok SZ, Koh C, *et al*. Parkin protects against LRRK2 G2019S mutant-induced dopaminergic neurodegeneration in Drosophila. *J Neurosci* 2009;**29**:11257–62.
91. **Venderova K,** Kabbach G, Abdel-Messih E, *et al*. Leucine-rich repeat kinase 2 interacts with parkin, DJ-1 and PINK-1 in a Drosophila melanogaster model of Parkinson's disease. *Hum Mol Genet* 2009;**18**:4390–404.
92. **Chan D,** Citro A, Cordy JM, *et al*. Rac1 protein rescues neurite retraction caused by G2019S leucine-rich repeat kinase 2 (LRRK2). *J Biol Chem* 2011;**286**:16140–9.
93. **Angeles DC,** Gan BH, Onstead L, *et al*. Mutations in LRRK2 increase phosphorylation of peroxiredoxin 3 exacerbating oxidative stress-induced neuronal death. *Hum Mutat* 2011;**32**:1390–7.
94. **Dusonchet J,** Kochubey O, Stafa K, *et al*. A rat model of progressive nigral neurodegeneration induced by the Parkinson's disease-associated G2019S mutation in LRRK2. *J Neurosci* 2011;**31**:907–12.
95. **Li X,** Wang QJ, Pan N, *et al*. Phosphorylation-dependent 14-3-3 binding to LRRK2 is impaired by common mutations of familial Parkinson's disease. *PLoS One* 2011;**6**: e17153.
96. **Najim al-Din AS,** Wriekat A, Mubaidin A, *et al*. Pallido-pyramidal degeneration, supranuclear upgaze paresis and dementia: Kufor-Rakeb syndrome. *Acta Neurol Scand* 1994;**89**:347–52.
97. **Ramirez A,** Heimbach A, Grundemann J, *et al*. Hereditary parkinsonism with dementia is caused by mutations in ATP13A2, encoding a lysosomal type 5 P-type ATPase. *Nat Genet* 2006;**38**:1184–91.
98. **Gitler AD,** Chesi A, Geddie ML, *et al*. Alpha-synuclein is part of a diverse and highly conserved interaction network that includes PARK9 and manganese toxicity. *Nat Genet* 2009;**41**:308–15.
99. **Ugolino J,** Fang S, Kubisch C, *et al*. Mutant Atp13a2 proteins involved in parkinsonism are degraded by ER-associated degradation and sensitize cells to ER-stress induced cell death. *Hum Mol Genet* 2011;**20**:3565–77.
100. **Tan J,** Zhang T, Jiang L, *et al*. Regulation of intracellular manganese hemeostasis by kufor-rakeb syndrome associated ATP13A2. *J Biol Chem* 2011;**286**:29654–62.
101. **Kawamoto Y,** Kobayashi Y, Suzuki Y, *et al*. Accumulation of HtrA2/Omi in neuronal and glial inclusions in brains with alpha-synucleinopathies. *J Neuropathol Exp Neurol* 2008;**67**:984–93.
102. **Kruger R,** Sharma M, Riess O, *et al*. A large-scale genetic association study to evaluate the contribution of Omi/HtrA2 (PARK13) to Parkinson's disease. *Neurobiol Aging* 2011;**32**:548 e9–18.
103. **Suzuki Y,** Takahashi-Niki K, Akagi T, *et al*. Mitochondrial protease Omi/HtrA2 enhances caspase activation through multiple pathways. *Cell Death Differ* 2004;**11**:208–16.
104. **Martins LM.** The serine protease Omi/HtrA2: a second mammalian protein with a reaper-like function. *Cell Death Differ* 2002;**9**:699–701.
105. **Martins LM,** Morrison A, Klupsch K, *et al*. Neuroprotective role of the reaper-related serine protease HtrA2/Omi revealed by targeted deletion in mice. *Mol Cell Biol* 2004;**24**:9848–62.
106. **Li B,** Hu Q, Wang H, *et al*. Omi/HtrA2 is a positive regulator of autophagy that facilitates the degradation of mutant proteins involved in neurodegenerative diseases. *Cell Death Differ* 2010;**17**:1773–84.
107. **Morgan NV,** Westaway SK, Morton JE, *et al*. PLA2G6, encoding a phospholipase A2, is mutated in neurodegenerative disorders with high brain iron. *Nat Genet* 2006;**38**:752–4.
108. **Paisan-Ruiz C,** Bhatia KP, Li A, *et al*. Characterization of PLA2G6 as a locus for dystonia-parkinsonism. *Ann Neurol* 2009;**65**:19–23.
109. **Yoshino H,** Tomiyama H, Tachibana N, *et al*. Phenotypic spectrum of patients with PLA2G6 mutation and PARK14-linked parkinsonism. *Neurology* 2010;**75**:1356–61.
110. **Jenkins CM,** Wolf MJ, Mancuso DJ, *et al*. Identification of the calmodulin-binding domain of recombinant calcium-independent phospholipase A2beta. Implications for structure and function. *J Biol Chem* 2001;**276**:7129–35.
111. **Wang Z,** Ramanadham S, Ma ZA, *et al*. Group VIA phospholipase A2 forms a signaling complex with the calcium/calmodulin-dependent protein kinase IIbeta expressed in pancreatic islet beta-cells. *J Biol Chem* 2005;**280**:6840–9.
112. **Shojaee S,** Sina F, Banihosseini SS, *et al*. Genome-wide linkage analysis of a Parkinsonian-pyramidal syndrome pedigree by 500 K SNP arrays. *Am J Hum Genet* 2008;**82**:1375–84.
113. **Di Fonzo A,** Dekker MC, Montagna P, *et al*. FBXO7 mutations cause autosomal recessive, early-onset parkinsonian-pyramidal syndrome. *Neurology* 2009;**72**:240–5.
114. **Pankratz N,** Wilk JB, Latourelle JC, *et al*. Genomewide association study for susceptibility genes contributing to familial Parkinson disease. *Hum Genet* 2009;**124**:593–605.
115. **Edwards TL,** Scott WK, Almonte C, *et al*. Genome-wide association study confirms SNPs in SNCA and the MAPT region as common risk factors for Parkinson disease. *Ann Hum Genet* 2010;**74**:97–109.
116. **Hamza TH,** Zabetian CP, Tenesa A, *et al*. Common genetic variation in the HLA region is associated with late-onset sporadic Parkinson's disease. *Nat Genet* 2010;**42**:781–5.
117. **Spencer CC,** Plagnol V, Strange A, *et al*. Dissection of the genetics of Parkinson's disease identifies an additional association 5' of SNCA and multiple associated haplotypes at 17q21. *Hum Mol Genet* 2010;**20**:345–53.
118. **Liu X,** Cheng R, Verbitsky M, *et al*. Genome-wide association study identifies candidate genes for Parkinson's disease in an Ashkenazi Jewish population. *BMC Med Genet* 2011;**12**:104.
119. **Do CB,** Tung JY, Dorfman E, *et al*. Web-based genome-wide association study identifies two novel Loci and a substantial genetic component for Parkinson's disease. *PLoS Genet* 2011;**7**:e1002141.
120. **Hruska KS,** Goker-Alpan O, Sidransky E. Gaucher disease and the synucleinopathies. *J Biomed Biotechnol* 2006;**2006**:78549.
121. **Sidransky E,** Nalls MA, Aasly JO, *et al*. Multicenter analysis of glucocerebrosidase mutations in Parkinson's disease. *N Engl J Med* 2009;**361**:1651–61.
122. **Aharon-Peretz J,** Rosenbaum H, Gershoni-Baruch R. Mutations in the glucocerebrosidase gene and Parkinson's disease in Ashkenazi Jews. *N Engl J Med* 2004;**351**:1972–7.
123. **Mata IF,** Samii A, Schneer SH, *et al*. Glucocerebrosidase gene mutations: a risk factor for Lewy body disorders. *Arch Neurol* 2008;**65**:379–82.
124. **De Marco EV,** Annesi G, Tarantino P, *et al*. Glucocerebrosidase gene mutations are associated with Parkinson's disease in southern Italy. *Mov Disord* 2008;**23**:460–3.
125. **Morris HR,** Lees AJ, Wood NW. Neurofibrillary tangle parkinsonian disorders—tau pathology and tau genetics. *Mov Disord* 1999;**14**:731–6.
126. **Galpern WR,** Lang AE. Interface between tauopathies and synucleinopathies: a tale of two proteins. *Ann Neurol* 2006;**59**:449–58.
127. **Tayebi N,** Walker J, Stubblefield B, *et al*. Gaucher disease with parkinsonian manifestations: does glucocerebrosidase deficiency contribute to a vulnerability to parkinsonism? *Mol Genet Metab* 2003;**79**:104–9.
128. **Goker-Alpan O,** Stubblefield BK, Giasson BI, *et al*. Glucocerebrosidase is present in alpha-synuclein inclusions in Lewy body disorders. *Acta Neuropathol* 2010;**120**:641–9.
129. **Cullen V,** Sardi SP, Ng J, *et al*. Acid beta-glucosidase mutants linked to Gaucher disease, Parkinson disease, and Lewy body dementia alter alpha-synuclein processing. *Ann Neurol* 2011;**69**:940–53.
130. **Yap TL,** Gruschus JM, Velayati A, *et al*. Alpha-synuclein interacts with glucocerebrosidase providing a molecular link between Parkinson and Gaucher diseases. *J Biol Chem* 2011;**286**:28080–8.
131. **Hardy J.** No definitive evidence for a role for the environment in the etiology of Parkinson's disease. *Mov Disord* 2006;**21**:1790–1.
132. **Deng X,** Dzamko N, Prescott A, *et al*. Characterization of a selective inhibitor of the Parkinson's disease kinase LRRK2. *Nat Chem Biol* 2011;**7**:203–5.

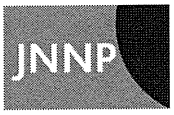

# Molecular pathogenesis of Parkinson's disease: update

Shinji Saiki, Shigeto Sato and Nobutaka Hattori

*J Neurol Neurosurg Psychiatry* published online December 3, 2011
doi: 10.1136/jnnp-2011-301205

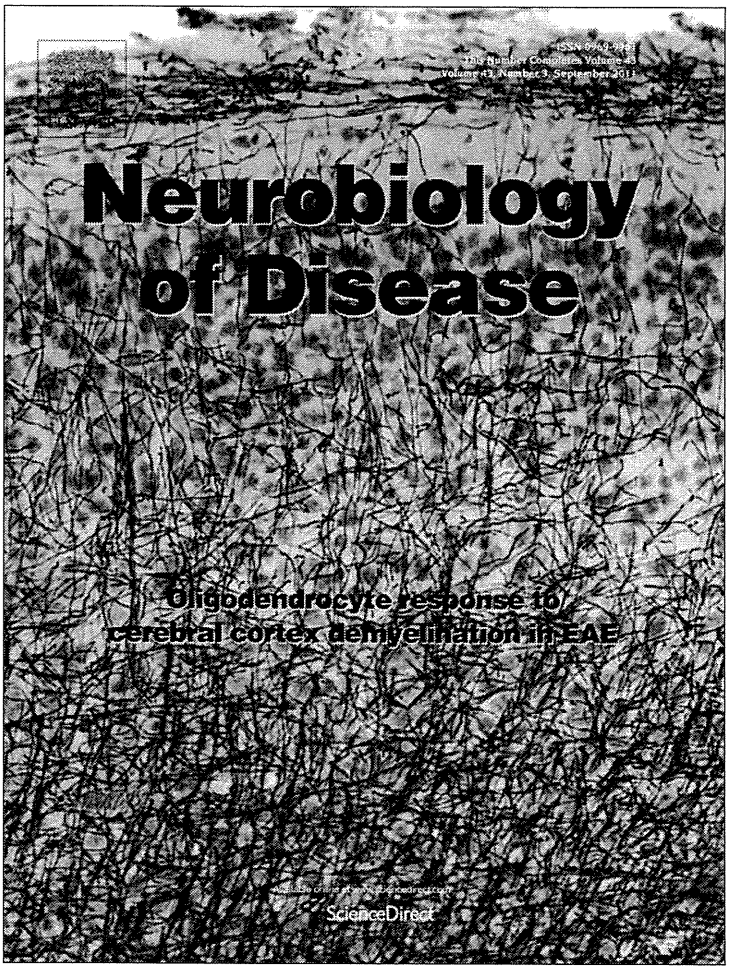

Neurobiology of Disease 43 (2011) 651–662

Contents lists available at ScienceDirect

Neurobiology of Disease

journal homepage: www.elsevier.com/locate/ynbdi

# DJ-1 associates with synaptic membranes

Yukiko Usami [a], Taku Hatano [a], Satoshi Imai [b,1], Shin-ichiro Kubo [a], Shigeto Sato [a], Shinji Saiki [a], Yoichiro Fujioka [c], Yusuke Ohba [c], Fumiaki Sato [b,2], Manabu Funayama [a,b], Hiroto Eguchi [a], Kaori Shiba [b], Hiroyoshi Ariga [d], Jie Shen [e], Nobutaka Hattori [a,b,*]

[a] Department of Neurology, Juntendo University School of Medicine, Japan
[b] Research Institute for Diseases of Old Age, Graduate School of Medicine, Juntendo University, Japan
[c] Laboratory of Pathophysiology and Signal Transduction, Hokkaido University Graduate School of Medicine, Japan
[d] Graduate School of Pharmaceutical Sciences, Hokkaido University, Japan
[e] Center for Neurologic Diseases, Brigham and Women's Hospital Program in Neuroscience, Harvard Medical School, USA

ARTICLE INFO

*Article history:*
Received 6 February 2011
Revised 30 April 2011
Accepted 20 May 2011
Available online 30 May 2011

*Keywords:*
DJ-1
Parkinson's disease
Localization
Synaptic vesicles
Synaptophysin
VAMP2
Rab3A

ABSTRACT

Parkinson's disease (PD) is a neurodegenerative disorder caused by loss of dopaminergic neurons. Although many reports have suggested that genetic factors are implicated in the pathogenesis of PD, molecular mechanisms underlying selective dopaminergic neuronal degeneration remain unknown. *DJ-1* is a causative gene for autosomal recessive form of *PARK7*-linked early-onset PD. A number of studies have demonstrated that exogenous DJ-1 localizes within mitochondria and the cytosol, and functions as a molecular chaperon, as a transcriptional regulator, and as a cell protective factor against oxidative stress. However, the precise subcellular localization and function of endogenous DJ-1 are not well known. The mechanisms by which mutations in DJ-1 contributes to neuronal degeneration also remain poorly understood. Here we show by immunocytochemistry that DJ-1 distributes to the cytosol and membranous structures in a punctate appearance in cultured cells and in primary neurons obtained from mouse brain. Interestingly, DJ-1 colocalizes with the Golgi apparatus proteins GM130 and the synaptic vesicle proteins such as synaptophysin and Rab3A. Förster resonance energy transfer analysis revealed that a small portion of DJ-1 interacts with synaptophysin in living cells. Although the wild-type DJ-1 protein directly associates with membranes without an intermediary protein, the pathogenic L166P mutation of DJ-1 exhibits less binding to synaptic vesicles. These results indicate that DJ-1 associates with membranous organelles including synaptic membranes to exhibit its normal function.



## Introduction

Parkinson's disease (PD) is the second most common neurodegenerative disorder next to Alzheimer's disease and is characterized by motor symptoms as cardinal features such as resting tremor, rigidity, bradykinesia and postural instability. Pathological hallmarks of PD include marked cell loss of dopaminergic neurons in the substantia nigra pars compacta which causes dopamine depletion in the striatum and the presence of intracytoplasmic inclusions known as Lewy bodies in the remaining neurons (Fearnley and Lees, 1991). Although most of the PD cases are sporadic, approximately 5% of PD patients have clear familial etiology. Thus, the presence of monogenic forms of familial PD tells us that genetic factors contribute to the pathogenesis of PD. Indeed, heterozygous and homozygous mutations in one of the responsible genes have been reported in sporadic cases, suggesting that genetic factors are implicated in the pathogenesis of PD. Until now, 9 genes for familial PD have been reported, and these include *α-synuclein*, *parkin*, *UCH-L*, *PINK-1*, *DJ-1*, *LRRK2*, *ATP13A2*, *PLA2G6*, and *FBXO7* (Hatano et al., 2009).

Previous reports have suggested that DJ-1 functions as a molecular chaperon (Lee et al., 2003), a transcriptional regulator (Kim et al., 2005; Niki et al., 2003; Shinbo et al., 2005; Takahashi et al., 2001), and as a cell protective factor against oxidative stress (Canet-Aviles et al., 2004; Taira et al., 2004b; Yokota et al., 2003). The localization of DJ-1 has been shown to be in mitochondria, cytosol, nucleus, and microsomes (endoplasmic reticulum (ER) and Golgi) (Bonifati et al., 2003; Canet-Aviles et al., 2004; Miller et al., 2003; Taira et al., 2004a). However, most studies have been performed by exogenous DJ-1 using overexpression systems. On the other hand, endogenous DJ-1 is present in synaptic terminals, in both axons and dendrites, as well as

*Abbreviations:* PD, Parkinson's disease; FRET, Förster resonance energy transfer; WT, wild type; ER, endoplasmic reticulum; KO, knockout; RT, room temperature; PBS, phosphate-buffer saline; FBS, fetal bovine serum; BSA, bovine serum albumin; Tfn-R, transferrin receptor; IR, immunoreactivity; HB, homogenizing buffer.

* Corresponding author at: Department of Neurology, Juntendo University School of Medicine, 2-1-1 Hongo, Bunkyo-ku, Tokyo 113-8421, Japan. Fax: +81 3 5800 0547.
*E-mail address:* nhattori@juntendo.ac.jp (N. Hattori).
[1] Present affiliation: Department of Toxicology, School of Pharmacy and Pharmaceutical Sciences, Hoshi University, Japan.
[2] Present affiliation: Department of Clinical Chemistry, School of Pharmacy and Pharmaceutical Sciences, Hoshi University, Japan.

**Available online on ScienceDirect (www.sciencedirect.com).**

0969-9961/$ – see front matter © 2011 Elsevier Inc. All rights reserved.
doi:10.1016/j.nbd.2011.05.014

in mitochondria (Olzmann et al., 2007; Zhang et al., 2005). However, the precise function and dynamics of DJ-1 related to vesicular trafficking remain unclear. In the present study, we demonstrate the association of endogenous DJ-1 with membranous organelles and the molecular interaction of recombinant DJ-1 protein with membranes in cultured cells. In addition, we examine whether pathogenic mutations found in *PARK7*-linked early onset PD patients may be affected by binding activities of DJ-1.

## Materials and methods

### *Antibodies and recombinant proteins*

Mouse monoclonal antibody (M043-3, Clone 3E8) and rabbit polyclonal antibody (NB300-270) for DJ-1 were obtained from Medical & Biological Laboratories Co. (MBL, Nagoya, Japan) and Novus Biologicals, Inc. (Littleton, CO), respectively. Rabbit polyclonal antibodies to Rab3A (sc-308), Rab4A (sc-312), Rab5B (sc-598), and Tom20 (sc-11415) were purchased from Santa Cruz Biotechnology (Santa Cruz, CA), and Rab7B (R4779) was obtained from Sigma (St. Louis, MO). Mouse monoclonal antibodies to synaptophysin were purchased from Chemicon International, Inc. (MAB5258, Temecula, CA) (used for immunoblotting) and Progen Biotechnik (61012, Heidelberg, Germany) (used for immunocytochemistry). Synaptotagmin (610434) and NMDAR1 (556308) were obtained from BD Biosciences Pharmingen (San Diego, CA). Other primary antibodies were Rab3A (107111, Synaptic Systems, Gottingen, Germany), anti-human transferrin receptor (13-6800, Zymed Laboratories, South San Francisco, CA), Parkin (#4211) and Calnexin (#2679S) (Cell Signaling, Danvers, MA), VAMP2 (NB300-595, Novus Biologicals, Inc.), BIP2 (ab21685, Abcam, Cambridge, MA), Hsp70 (610608, BD Transduction Laboratories), Mito Tracker Red CMXRos (M-7512, Molecular Probes), and total OXPHOS rodent WB antibody cocktail (MS604; MitoSciences, Eugene, Oregon). Secondary antibodies conjugated to horseradish peroxidase were purchased from GE HealthCare Bio-Sciences (Piscataway, USA). From Invitrogen Molecular Probes, 488 and 546 conjugated secondary antibodies were purchased. The vectors encoding GST-tagged WT and mutants DJ-1 (M26I, A104T, D149A, and L166P) were kindly provided by Hiroyoshi Ariga (Laboratory of Pharmaceutical Science, Hokkaido University).

### *Experimental animals (DJ-1 KO mice)*

The DJ-1 KO mice (F2) were a kind gift from The Laboratory of Pharmaceutical Science, Hokkaido University. The DJ-1 KO mice were generated at the Center for Neurologic Diseases, Brigham and Women's Hospital Program in Neuroscience, Harvard Medical School (Goldberg et al., 2005). F2 progeny were backcrossed for five generations to C57BL/6 mice, and heterozygotes were intercrossed to generate homozygous mice for the targeted *DJ-1* allele. For the experiments, C57BL/6J mice and DJ-1 KO mice were used at 7 to 9 weeks of age. All animal experiments were carried out in accordance with the Ethics Review Committee for Animal Experimentation of Juntendo University School of Medicine.

### *Cell culture and transfection*

SH-SY5Y cells and HeLa cells were grown in Dulbecco's modified Eagle's medium (D-MEM, Sigma) with 10% fetal bovine serum (FBS; Sigma) and 1% penicillin–streptomycin (PS; Invitrogen). SH-SY5Y cell culture medium was supplemented with 1% non-essential amino acid, 1% sodium pyruvate, and 1% L-glutamate (Invitrogen). The cells were cultured at 37 °C and 5% $CO_2$. PC12 cells were grown in D-MEM with 5% FBS and 10% horse serum. Primary cortical neurons containing glia cells were prepared from E15.5 C57BL/6J mice and cultured for growth on Fisher-brand cover glass (Fisher Scientific, Pittsburgh, USA) in starting medium (F12 and Minimum Essential Medium with 10% FBS, 1% PS, and 0.001% insulin) for 3 days, and incubated sequentially for 5 days with 0.5 μM Ara-C (Sigma) in maintenance medium (F12 and Minimum Essential Medium with 5% calf serum, 5% horse serum, 1% PS, and 0.001% insulin). HeLa cells were transfected with expression vectors for FLAG-DJ-1 WT, M26I, A104T, D149A, or L166P by using FuGENE HD Transfection Reagent (Roche). After 24 h, immunocytochemistry was performed on the cells.

### *Immunocytochemistry*

Cells were fixed for 10 min in 4% paraformaldehyde and 0.5% sucrose in phosphate-buffered saline (PBS). The cells were permeabilized with PBS containing 0.2% Triton X-100 (Sigma) for 5 min at RT. For blocking, 1× BlockAce (Yukijirushi Co., Osaka, Japan) was used for SH-SY5Y cells, and 10% FBS and 1% bovine serum albumin (BSA) in PBS (primary cortical neurons from mice) was used for primary cortical neurons for 30 min. Cells were incubated overnight with primary antibodies at 4 °C. The cells were washed 3 times with PBS and were incubated at RT for 1 h with secondary antibodies. After the cells were washed 3 times with PBS, the slides were mounted with Vectashield (Vector Laboratories, Burlingame, CA) and analyzed using a Leica confocal microscopy.

### *Preparation of synaptosome fractions from mouse brain*

Synaptic vesicles were prepared as described previously (Hatano et al., 2007; Hell, 1998), with some modification. Briefly, whole brains from 3 mice (C57BL/6J) at 7 to 9 weeks of age were placed into 8 ml ice-cold synaptosomal homogenizing buffer (HB) (0.32 M sucrose, 4 mM HEPES–NaOH, pH 7.4 with EDTA-free protease inhibitor cocktail Complete Mini, EDTA free). The tissues were homogenized using a glass-Teflon homogenizer (10 up and down strokes, 830 rpm). The homogenized brain sample was centrifuged at 1000*g* for 10 min at 4 °C. After the supernatant (S1-1) was removed, the pellet was re-suspended in 5 ml HB and was homogenized and centrifuged at the same speed. The supernatant (S1-2) was removed, and the pellet was resuspended in 3 ml HB, and was homogenized and centrifuged in the same manner. The pellet was considered the P1 fraction, while the supernatant (mixed with S1-1, S1-2, and S1-3) was centrifuged at 12,000*g* for 15 min at 4 °C. The supernatant (S2) was removed and the pellet (P2) was resuspended with HB, and then centrifuged for 15 min at 13,000*g* at 4 °C. After removal of the supernatant (S2′), the pellet (P2′) was collected as the crude synaptosome fraction. P2′ was subsequently re-suspended with HB to a final volume of 1 ml. The P2′ fraction was suspended with 4 ml of ice cold water in the EDTA-free protease inhibitor cocktail. The samples were homogenized by 6 up and down strokes of the glass-Teflon homogenizer at 830 rpm and mixed with 39 μl 1 M HEPES, pH 7.4, then centrifuged for 20 min at 33,000*g* at 4 °C. The lysate pellet was considered the LP1 fraction, and the supernatant (LS1) was centrifuged for 2 h at 260,000*g* at 4 °C. After the supernatant (LS2) was removed, the pellet (LP2) was resuspended with 300 μl of HB. To loosen the pellet, samples were extruded consecutively through a 23-gauge and a 26-gauge hypodermic needle attached to a 1 ml syringe. The concentration of protein in each of the fractions was calculated using the BCA protein assay kit (Pierce, Rockford, IL). Finally, the same amounts of proteins from each fraction were analyzed by SDS–PAGE followed by immunoblotting.

### *Sucrose gradients of LS1 fraction from mouse brain*

The LS1 fraction was layered on top of a linear sucrose density gradient ranging from 0.2 to 2.0 M sucrose dissolved in HEPES buffer (pH 7.4), and ultra-centrifuged at 465,000*g* for 13 h at 4 °C. Each of the fractions (0.5 ml) was collected from the top of the gradient, and equal volumes of each fraction were subjected to SDS–PAGE followed by immunoblotting.

*Preparation of magnetic beads cross-linked with antibodies*

For the following experiments of immunoisolation and immunoprecipitation, the DJ-1 polyclonal antibody and the synaptophysin antibody, and the normal rabbit IgG and the normal mouse IgG as control, were cross-linked to protein G-coated magnetic beads (Dynabeads Invitrogen). The beads were washed 3 times with citrate buffer, and then 50 μl of magnetic bead slurry was combined with 50 μg of each antibody by rotating for 1 h at RT. The antibody-bound beads were washed 3 times with 0.2 M sodium borate buffer (pH 9.0), and then resuspended in 0.2 M sodium borate buffer containing dimethyl pimelimidate (Pierce Biotechnology). After reacting by rotating the samples for 1 h at RT, the supernatants were removed and the Dynabead pellets were washed 3 times with 0.2 M triethanolamine buffer (pH 8.0). The washed beads were suspended with 0.2 M triethanolamine buffer containing 50 mM glycine, and were reacted for 2 h at RT. The supernatant was removed and the beads were washed 3 times with PBS, stored at 4 °C with PBS containing 0.05% Tween 20, and used within 1 week of the reactions.

*Immunoisolation and immunoprecipitation of LS1 fraction containing synaptic vesicles from the mouse brain*

Immunoisolation: beads cross-linked with DJ-1 antibody and synaptophysin antibody, or beads cross-linked with normal rabbit IgG and normal mouse IgG were washed 6 times with PBS and were blocked for 1 h at RT using PBS containing 10% BSA as nonspecific competitor, followed by washing in PBS 3 times. In addition, each of the 1 ml LS1 fraction samples were immunoisolated with 37.5 μl of the beads cross-linked with antibody for a total of 12 h at 4 °C after blocking non-specific sites by rotating with the beads with the cross-linked normal rabbit IgG, or normal mouse IgG for 1 h at 4 °C. The pellets and supernatants were subjected to SDS–PAGE followed by immunoblotting using antibodies against the indicated proteins.

Immunoprecipitation: beads cross-linked with the antibodies, the same as in the immunoisolation protocol, were blocked using PBS containing 10% BSA for 1 h at RT. LS1 fractions (900 μl) were dissolved in 100 μl of 10× RIPA buffer (final concentration: 140 mM KCl, 20 mM HEPES–KOH (pH 7.3), 2 mM EDTA, protease inhibitors, and 1% Triton X-100), and then the samples were blocked by rotating with normal IgG for 1 h at 4 °C. The supernatants were immunoprecipitated with 12.5 μl of each of the beads cross-linked with antibody overnight at 4 °C. The pellets and supernatants were subjected to SDS–PAGE followed by immunoblotting using antibodies against the indicated proteins.

*Förster resonance energy transfer (FRET)*

Synaptophysin-YFP and pCAGGS-CFP vector were a kind of gift from the Department of Cellular Neurobiology Graduate School of Medicine University of Tokyo. CFP–DJ-1 and CFP–VAMP2 were generated by fusing in frame to the DJ-1 N-terminal or VAMP2 N-terminal coding region in the pCAGGS-CFP vector. HeLa cells were transfected with expression vectors for CFP–DJ-1 or CFP–VAMP2, and synaptophysin-YFP using FuGene HD (Roche), according to the manufacturer's instruction. After 24 h, the cells were imaged with an IX70 inverted microscope (Olympus, Tokyo, Japan) equipped with BioPoint MAC5000 excitation and emission filter wheels (Ludl Electronic Products Ltd., Hawthorne, NY) and a Cool SNAP-HQ cooled CCD camera (Roper Scientific, Trenton, NJ). The filters used were purchased from Omega Optical Inc. (Brattleboro, VT): two excitation filters, XF1071 (440AF21) for CFP and Förster resonance energy transfer (FRET), and XF1068 (500AF25) for YFP; an XF2034 (455DRLP) dichroic mirror; two emission filters, XF3075 (480AF30) for CFP and XF3079 (535AF26) for FRET and YFP. Cells were illuminated with a 75 W xenon lamp through a 6% ND filter. Exposure times for 3×3 binning were 100 ms to obtain fluorescence images and 20 ms to obtain differential interference contrast image. MetaMorph software (Universal Imaging, West Chester, PA) was used to control the CCD camera and filter wheels, and also for the analysis of the cell image data.

Sensitized FRET measurement was performed using the method by Gordon et al.(1998). Briefly, fluorescence images for more than 20 cells were acquired sequentially through YFP, CFP, and FRET filter channels. The background was subtracted from raw images before FRET calculations. The fractions of the bleed-through of CFP and YFP fluorescence through the FRET channel were 0.502 and 0.385, respectively. Corrected FRET ($FRET_C$) was therefore calculated on a pixel-by-pixel basis for the entire image by using the equation: $FRET_C = FRET - 0.502 \times CFP - 0.385 \times YFP$, where FRET, YFP, and CFP correspond to background-subtracted images of cells co-expressing CFP and YFP. Calculated $FRET_C$ values are expressed as box and whisker plots, where the highest and lowest boundaries of the box represent the 25th and 75th percentiles, respectively, and whiskers above and below the box designate the 10th and 90th percentiles, respectively; the line within the box indicates the median value. $FRET_C$ images are also presented in the pseudocolor mode.

Alternatively, 293F cells (Invitrogen) were transfected with expression vectors for CFP–DJ-1 or CFP–VAMP2, and synaptophysin-YFP using 293fectin (Invitrogen) according to the manufacturer's recommendation. After 24 h, the cells were analyzed by a Flicyme-300 flow cytometer (Mitsui engineering and Shipment, Tokyo, Japan), which is equipped with a 445 nm semiconductor laser and is able to measure the fluorescence lifetime of CFP in the frequency domain at a single cell level. Data were acquired using the machine-bundled software, and exported to FlowJo flow cytometry analysis software (Tree Star, Inc., Ashland, OR). Using a gate tool, a population that expresses both CFP and YFP was selected, and FRET efficiency ($E$) of each cell was calculated by the following equation: $E = 1 - \tau_d'/\tau_d$, where, $\tau_d'$ and $\tau_d$ are donor (CFP) lifetimes in the presence and absence of the acceptor chromophore, respectively. $E$ values of all analyzed cells were plotted in box and whisker plots.

*Confocal laser scanning microscopy*

Confocal images were obtained using an FV-10i confocal microscope (Olympus, Tokyo, Japan). Image data were exported to MetaMorph software and fluorescence intensities on lines of interest were gauged by the "Line Scan" function and plotted.

*Cell fractionation*

For cell fractionation studies, cultured cells (PC12) were washed with PBS, scraped off the culture plate in PBS, and centrifuged at 600*g* for 5 min. Cell pellets were resuspended in homogenization buffer (20 mM HEPES pH 7.2 and 0.25 M sucrose) in the presence of a cocktail of protease inhibitor (Complete Mini, EDTA-free), and sonicated at 4 °C (10 s, 3 times). The nuclei and unbroken cells were then pelleted by centrifugation at 1000*g* for 10 min at 4 °C. The supernatant was centrifuged at 100,000*g* for 1 h at 4 °C to separate the cytosolic and membrane fractions. To study the effects of salts and non-ionic detergent on the solubilization of DJ-1, the membrane fractions were incubated on ice for 30 min with homogenization buffer with 50, 150, and 1000 mM sodium chloride or 1% Triton X-100. After separation of the soluble and insoluble materials by centrifugation (100,000g, for 1 h, at 4 °C), equal volumes of each fraction were subjected to immunoblot with DJ-1, Parkin, and Tfn-R antibodies.

*Proteinase K (PK) digestion of PC12 cell membrane fractions*

Membrane fractions were isolated from PC12 cells and incubated with 0, 20, 40, 60, 80, and 120 μl of Proteinase K (PK)-agarose (Sigma) at 30 °C with rotation for 1 h. PK beads were removed from the